ISSN 1023-9855

胸腔醫學

Thoracic Medicine

The Official Journal of Taiwan Society of Pulmonary and Critical Care Medicine

Vol.28 No.1 Feb. 2013

第二十八卷 第一期

中華民國一〇二年二月

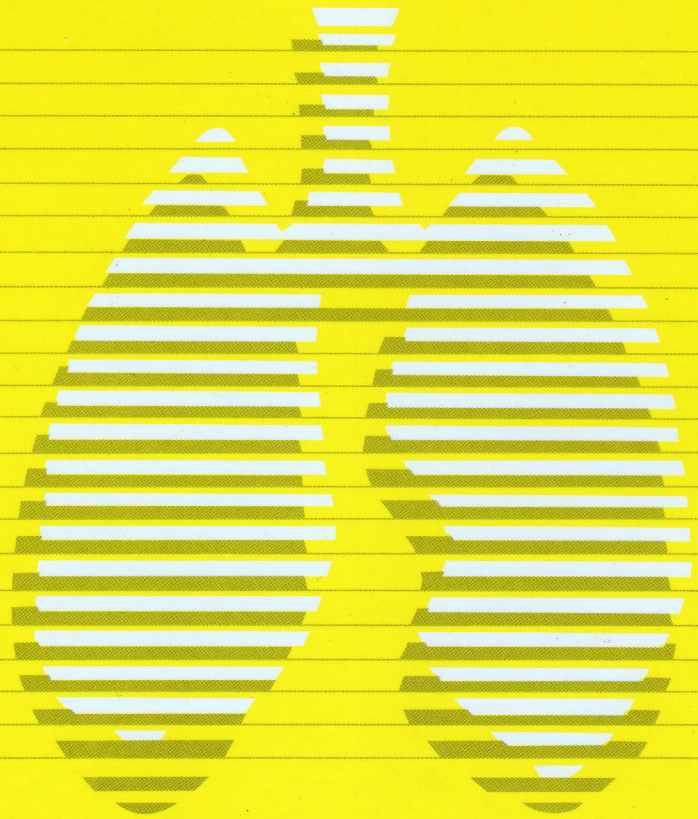

台灣胸腔暨重症加護醫學會

11217 台北市北投區石牌路二段201號

5.No.201, Sec. 2, Shipai Rd., Beitou District, Taipei City, Taiwan 11217, R.O.C.

ISSN 1023-9855

中華民國一〇二年二月　第二十八卷　第一期

ISSN 1023－9855

胸腔醫學

Thoracic Medicine

The Official Journal of Taiwan Society of Pulmonary and Critical Care Medicine

Vol.28 No.1 February 2013

原著

卡斯托曼病在南臺灣一醫院之經驗.....1~7
連啟惇，周世華，吳俊杰，黃明賢，楊志仁

傳統電腦斷層和正子掃瞄在非小細胞癌診斷分期上的準確度分析比較.....8~17
徐稟智，陳志弘，何恭之，吳怡成，高國晉，劉劍英，張文震，蔡熒煌，楊政達

病例報告

老年病人肺泡蛋白沉積症合併肺麴菌感染：病例報告與文獻回顧.....18~24
鄒秉誠，傅彬貴，陳奕先，沈光漢，許正園

於呼吸器使用時，嚴重的皮下氣腫造成之致命的上呼吸道阻塞：個案報告.....25~30
高建華，余文光，連德正

氣管支氣管巨大症與僵直性脊椎炎：病例報告及文獻回顧.....31~37
韓孟志，張漢煜

診斷肺原發類淋巴上皮細胞癌上的陷阱－病例報告與文獻回顧.....38~43
吳宜謀，沈光漢，許正園

原發性支氣管內許旺細胞瘤併存同側肺腺癌：病例報告與文獻回顧.....44~50
詹博強，張竣期，林慶雄

罕見解剖構造異常引起阻塞性睡眠呼吸中止症－病例報告.....51~56
陳鈴宜，王景平，黃偉彰，吳明峰，許正園

肺泡蛋白沉積症的支氣管肺泡灌洗前後生理參數變化－病例報告.....57~64
曾健華，許正園，傅彬貴

中華民國一〇二年二月　第二十八卷　第一期

ISSN 1023－9855

Vol.28 No.1 February 2013

胸腔醫學
Thoracic Medicine

The Official Journal of Taiwan Society of Pulmonary and Critical Care Medicine

Orginial Articles

Castleman's Disease in a Single Institution in Southern Taiwan ..... 1~7
Chi-Tun Lien, Shah-Hwa Chou, Chun-Chieh Wu, Ming-Shyan Huang, Chih-Jen Yang

Efficacy Comparison of Conventional Computed Tomography and Whole-body ^{18}F-Fluorodeoxyglucose Positron Emission Tomography for Staging in Non-small Cell Lung Cancer Patients ..... 8~17
Ping-Chih Hsu, Chih-Hung Chen, Kung-Chu Ho, Yi-Chen Wu, Kuo-Chin Kao, Chien-Ying Liu, Wen-Cheng Chang, Ying-Huang Tsai, Cheng-Ta Yang

Case Reports

Pulmonary Alveolar Proteinosis Combined with Pulmonary Aspergillosis in an Elderly Patient: A Case Report and Literature Review ..... 18~24
Ping-Hsien Tsou, Pin-Kuei Fu, Yi-Hsien Chen, Gwan-Han Shen, Jeng-Yuan Hsu

Life-threatening Upper Airway Obstruction Caused by Massive Subcutaneous Emphysema during Mechanical Ventilation: A Case Report ..... 25~30
Jiann-Hwa Kao, Wen-Kuang Yu, Te-Cheng Lien

Tracheobronchomegaly and Ankylosing Spondylitis: A Case Report and Literature Review ..... 31~37
Meng-Zhi Han, Han-Yu Chang

Pitfall in Diagnosing Lymphoepithelioma-like Carcinoma of the Lung: A Case Report and Literature Review ..... 38~43
Yi-Mou Wu, Gwan-Han Shen, Jeng-Yuan Hsu

A Primary Endobronchial Schwannoma Coexisting with an Ipsilateral Lung Adenocarcinoma: A Case Report and Literature Review ..... 44~50
Po-Chiang Chan, Chun-Chi Chang, Ching-Hsiung Lin

Obstructive Sleep Apnea and Hypopnea Syndrome Originating from an Unusual Anatomical Obstructive Site – A Case Report ..... 51~56
Ling-I Chen, Ching-Ping Wang, Wei-Chang Huang, Ming-Feng Wu, Jeng-Yuan Hsu

Pulmonary Physiology before and after Bronchopulmonary Lavage for Pulmonary Alveolar Proteinosis – A Case Report ..... 57~64
Chien-Hua Tseng, Jeng-Yuan Hsu, Pin-Kuei Fu

Castleman's Disease in a Single Institution in Southern Taiwan

Chi-Tun Lien*,**, Shah-Hwa Chou***, Chun-Chieh Wu****, Ming-Shyan Huang**,*****, Chih-Jen Yang**,*****,******

Castleman's disease (CD) is a very rare lymphoproliferative disease, and the mediastinum is the most commonly involved site. Because of the rarity of CD, its etiology and pathogenesis are still uncertain. The initial impression of a CD-related mass is often that of a lymphoma, solitary malignancy, metastatic carcinoma or an infectious disease, rather than CD. The various types of CD are characterized by their distinctive lymphoid architectural changes in all nodal compartments, and can be divided into 4 types pathologically: unicentric, which has a hyaline vascular variant and a plasma cell variant, multicentric, and a new subtype, HHV-8-associated CD. The prognosis of CD depends on the subtype. The unicentric subtype usually has a good prognosis; however, recurrence or coexistence with malignancies or malignant sequelae is possible. In order to investigate this rare disease and its prognosis, we retrospectively reviewed all patients with CD with pathologically proven samples at Kaohsiung Medical University Hospital from 1990 to 2010. Five cases were recorded, all of which were of the unicentric type and hyaline vascular variant. The diagnoses were made based on surgical excisions, and no cases of recurrence were found after at least 1 year of follow-up, indicating the good prognosis. We present our case review and discuss the findings. ***(Thorac Med 2013; 28: 1-7)***

Key words: Castleman's disease, unicentric, hyaline-vascular type

Introduction

Castleman's disease (CD) is an uncommon lymphoproliferative disease that was first described by Benjamin in 1956 [1]. The etiology and pathogenesis are still uncertain. Chronic low-grade inflammation, a hamartomatous process, immunodeficiency and autoimmunity have

*Department of Internal Medicine, Kaohsiung Municipal United Hospital, Kaohsiung, Taiwan; **Division of Pulmonary Medicine, Department of Internal Medicine, Kaohsiung Medical University Hospital, Kaohsiung Medical University, Taiwan; ***Division of Chest Surgery, Department of Surgery, Kaohsiung Medical University Hospital, Kaohsiung Medical University, Taiwan; ****Department of Pathology, Kaohsiung Medical University Hospital, Kaohsiung Medical University, Taiwan; *****Department of Internal Medicine, Faculty of Medicine, College of Medicine, Kaohsiung Medical University, Taiwan; ******Department of Internal Medicine, Kaohsiung Municipal Ta-Tung Hospital, Kaohsiung Medical University, Kaohsiung, Taiwan
Address reprint requests to: Dr. Chih-Jen Yang, Division of Pulmonary Medicine, Department of Internal Medicine, Kaohsiung Medical University Hospital, Kaohsiung Medical University, Taiwan, #100, Tzyou 1st Road, Kaohsiung City, Taiwan

all been proposed as likely mechanisms [2]. In addition, infections such as Epstein-Barr virus, toxoplasma, and *Mycobacterium tuberculosis* have been noted in patients with CD, and may also be possible mechanisms. The mediastinum is most commonly involved (70%), followed by the neck, abdomen and axillae [3]. The various types of CD are characterized by distinctive lymphoid architectural changes in all nodal compartments, and can be divided into 4 types pathologically: unicentric, which has a hyaline vascular variant and a plasma cell variant, multicentric, and a new subtype, HHV-8-associated CD [4]. The unicentric type is the most common, accounting for approximately 80~90% of all cases of CD, and the hyaline vascular variant is the most common variant of the unicentric type, characterized by distinctive follicles with expanded mantle zones of small lymphocytes forming concentric rings surrounding 1 or more atresic germinal centers. The plasma cell variant is less common [5], is characterized by marked paracortical plasmacytosis, and occurs more commonly in the multicentric type of CD. Patients with the unicentric type of CD often exhibit no symptoms or only lymphadenopathy. They can often be treated surgically and usually have a good prognosis [6]. However, recurrence, and the coexistence of unicentric CD with malignancies or malignant sequelae after surgical resection have been reported [7-8]. The multicentric type, accounting for approximately 10~20% of all cases of CD, is histopathologically characterized by a massive accumulation of polyclonal plasma cells in the interfollicular region. This type of CD often has clinical findings, including generalized lymphadenopathy, fever, night sweats, malaise, splenomegaly, hypergammaglobulinemia, and cytopenias such as anemia and thrombocytopenia [9-10]. The multicentric type often has a more aggressive clinical course with the potential for malignant transformation and a poor outcome [11].

The purpose of this study was to investigate all of the pathologically proven cases of CD during the last 20 years in a tertiary teaching hospital in southern Taiwan, document the clinical presentations, tumor location, size, therapy and outcomes in the past 20 years, and perform a literature review.

Materials and Methods

Using a computer-assisted search of medical records, we retrospectively reviewed all cases with a definite diagnosis of CD at Kaohsiung Medical University Hospital (a 1,600-bed tertiary teaching hospital), in Kaohsiung, Taiwan from January 1990 to December 2010. Pathologically proven cases of CD were defined as those having a specific pathological feature observed by a pathologist and verified through a peer review. We recorded the types of CD, including unicentric and multicentric, and variants including hyaline vascular and plasma cell. We also carefully documented the basic information, clinical presentations, diagnostic methods, treatment and prognosis.

Results

Only 5 patients with CD were identified in the hospital records of the last 20 years. There was a female predominance, and the mean age was 48.4 years (range, 24~79 years). Two patients presented with an asymtomatic mass in the mediastinum that was unexpectedly noted on chest x-rays (CXR) during a health check. Chest computerized tomography (CT) showed a prominent huge mass in the middle mediasti-

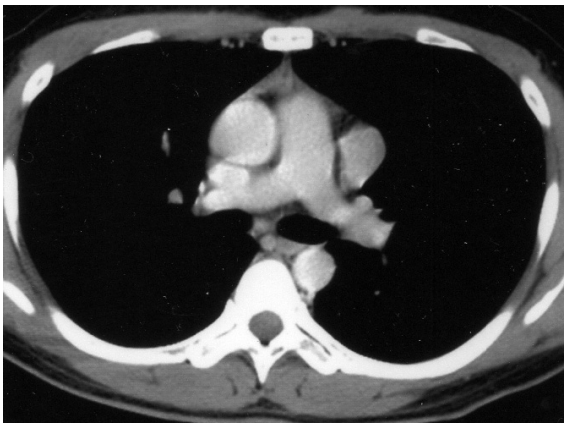

(A)

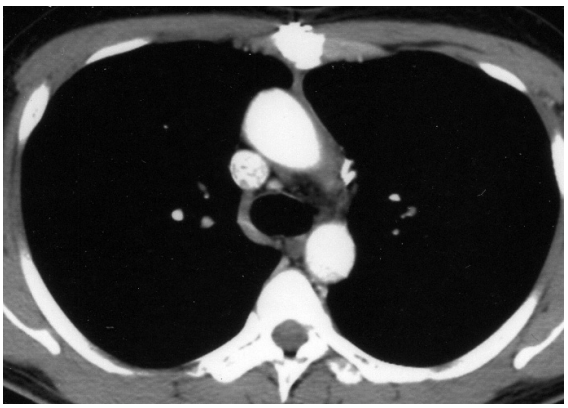

(B)

Fig. 1. Enhanced chest CT showed a homogeneous mass with moderate enhancement in the middle mediastinum in a patient (1A). No recurrence was noted after 1 year of follow-up (1B).

num with the initial impression of lymphoma in both patients (Figure 1). Two other patients had palpable masses in the neck for 2 weeks and 2 months, respectively. The remaining patient had a mass lesion in the inguinal area for 1 month. All of the patients had unicentric CD and the hyaline vascular variant (Figure 2); there were no cases of multicentric or plasma cell variant unicentric CD. All of the patients underwent successful surgical excision, and no evidence of tumor recurrence was noted after at least 1 year of follow-up, with the longest follow-up duration being 16 years. This indicates a good prognosis for unicentric CD with the hyaline vascular variant (Table 1).

Discussion

We documented all cases of CD in a tertiary teaching hospital in southern Taiwan from 1990 to 2010. All of the patients had the unicentric type of CD with the hyaline vascular variant, and they all underwent successful surgical excision. No recurrence within the first year of fol-

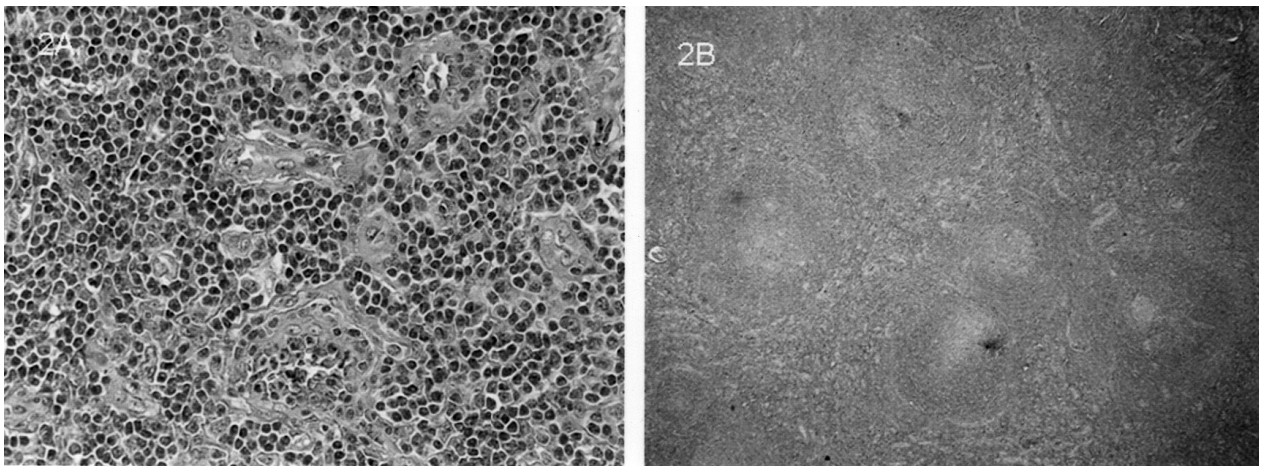

Fig. 2. Histopathological sections (hematoxylin & eosin stain) at 2 magnifications, original magnification x 100 (2A) and original magnification x 40 (2B), showed hyalinized vessels within germinal follicles that were surrounded by onion-like lymphocytes, indicating the typical features of the hyaline-vascular variant of CD.

Table 1. Summary of demographic and clinical findings and the prognosis of Castleman's Disease (CD) in Kaohsiung Medical University Hospital from 1990 to 2010

Patient NO.	Age/ gender	Subtype	Location	Initial presentations	Size (cm x cm x cm)	Therapy	Follow up and outcome
1	46/F	Unicentric Hyaline-vascular	Mediastinum	Nil (health exam)	4 x 3 x 3	Surgical excision	No more recurrence for 16 years
2	65/F	Unicentric Hyaline-vascular	Right inguinal area	A palpable mass over inguinal area for 1 month)	3 x 2 x 2	Surgical excision	No more recurrence for 11 years
3	24/F	Unicentric Hyaline-vascular	Right neck	A palpable mass over neck for 2 weeks	4.5 x 2.1 x 1	Surgical excision	No more recurrence for 5 years
4	79/F	Unicentric Hyaline-vascular	Left neck	A palpable mass over neck for 2 months	2.4 x 1.8 x 1.8	Surgical excision	No more recurrence for 3 years
5	28/M	Unicentric Hyaline-vascular	Mediastinum	Nil (health exam)	5.5 x 3 x 1	Surgical excision	No more recurrence for 1 years

low-up was noted, indicating a good prognosis.

CD is rare, and the unicentric type with the hyaline vascular variant is most common. Such patients are often asymptomatic [4]. Because of its rarity, the initial impression of a CD-related mass is often lymphoma [1], solitary malignancy [5,12-13], metastatic carcinoma [2,14] or an infectious disease [9-10,15], rather than CD. Contrast-enhanced CT is used routinely for the differential diagnosis [15] or follow-up, and the CD findings often show a homogeneous or heterogeneous mass of soft tissue attenuation [2,16]. Furthermore, ^{18}F-FDG PET imaging for CD has been proposed to be an effective tool for the initial assessment of disease extension, monitoring treatment, and the detection of recurrent disease, especially the multicentric type of CD [17].

The unicentric type of CD often needs nothing less than complete surgical excision [6]. These patients often have a good prognosis, as with our patients. However, if a particular case of the unicentric type of CD is unresectable, treatment strategies should be partial resection, external beam radiation therapy or observation alone [6,18]. Recurrence or the coexistence of CD with other malignancies or malignant sequelae in such cases is possible. Al-Saleh *et al* documented a unicentric type of CD in the retroperitoneum that was proven by an excisional biopsy [12]. The mass was extensively excised, and the final diagnosis showed the same pathological features as the biopsy. Chan *et al* reported a patient with the coexistence of unicentric CD and locally advanced papillary renal cell carcinoma [19]. Takehara *et al* reported a case with the coexistence of unicentric CD and a leiomyosarcoma in the retroperitoneum [20]. In addition, Bowne *et al* described a patient that had the unicentric type of CD with complete re-

section, but a large-cell malignant lymphoma of B-cell origin developed 1 year later [6]. Several similar reports have been documented and most of them involved lymphoma [7-8,21]. Therefore, careful follow-up is necessary. No disease recurrence was detected in any of our patients after complete resection.

Multicentric CD has been reported to have a high incidence of malignancies, especially lymphoma and Kaposi's sarcoma, reportedly involving 32% of patients with this type of CD [4,7,21]. Therapy is diverse and controversial. The most common treatments have been high-dose corticosteroids alone or combined with chemotherapy [6,22]. However, in some reports, the disease progressed rapidly and led to mortality, clearly indicating a poor prognosis. A multicentric type of CD has recently provided a new therapeutic target. Recognition of the role of interleukin-6 in disease perpetuation has led to the use of an antihuman interleukin-6 receptor monoclonal antibody, tocilizumab [23]. Rituximab, an anti-CD20 monoclonal antibody, targets CD20-positive B lymphocytes, a prominent component of this disorder [1]. Human herpes virus-8 and angiogenesis [4], both involved in the pathogenesis of CD, may provide additional unique therapeutic opportunities.

In summary, CD is a poorly understood disease that creates both diagnostic and therapeutic dilemmas for physicians. Complete surgical resection of unicentric disease at the time of presentation is likely to afford the best chance of a cure [6], as seen in our patients. Radiation therapy has been used with varied success in patients who are poor surgical candidates or in those with unresectable unicentric lesions [18]. Long-term follow-up is necessary due to possible malignant sequelae. In addition, multicentric CD has a higher incidence of malignant transformation and needs more aggressive treatment.

References

1. Dham A, Peterson BA. Castleman disease. Curr Opin Hematol 2007; 14: 354-9.
2. Baysungur V, Tezel C, Okur E, *et al*. An unusual presentation of Castleman's disease. Respiratol 2010; 15: 1012-4.
3. Lin CY, Chang YL. Castleman's disease in the head and neck region: Meta-analysis of reported cases in Taiwan and literature review. J Formos Med Assoc 2010; 109: 913-20.
4. Cronin DM, Warnke RA. Castleman disease: an update on classification and the spectrum of associated lesions. Adv Anat Pathol 2009; 16: 236-46.
5. Nistor C, Davidescue M, Ciuche A. A rare case of unicentric plasma cell type Castleman's disease in the mediastinum. Pneumologia 2010; 59: 32-5.
6. Bowne WB, Lewis JJ, Fillppa DA, *et al*. The management of unicentric and multicentric Castleman's disease: a report of 16 cases and a review of the literature. Cancer 1999; 85: 706-17.
7. Orcioni GF, Mambelli V, Ascani S. Concurrence of localized Castleman's disease and peripheral small B-lymphocytic lymphoma within the same lymph node. Gen Diagn Pathol 1998; 143: 327-30.
8. Vasef M, Katzin WE, Mendelsohn G. Report of a case of localized Castleman's disease with progression to malignant lymphoma. Am J Clin Pathol 1992; 98: 633-6.
9. Day JR, Bew D, Ali M, *et al*. Castleman's disease associated with myasthenia gravis. Ann Thorac Surg 2003; 75: 1648-50.
10. Rice BL, Farver CF, Pohlman B, *et al*. Concomitant Castleman's disease and sarcoidosis. Am J Med Sci 2011; 341: 257-9.
11. Abdel-Reheim FA, Koss W, Rappapart ES, *et al*. Coexistence of Hodgkin's disease and giant lymph node hyperplasia of the plasma-cell type (Castleman's disease). Arch Pathol Lab Med 1996; 120: 91-6.
12. Al-Saleh N, Itty P, Kukawski P, *et al*. Solitary intra-abdominal Castleman's disease, hyaline vascular type: case report. Gulf J Oncolog 2010; 7:53-6.
13. Wang SH, Ruan Z, Huang HL. A rare case of Castleman

disease presenting as pulmonary mass mimicking central pulmonary malignancy. Chin Med J 2009; 122: 990-1.
14. Hsu HH, Chen YC, Fang JT, *et al*. Unicentric Castleman's disease associated with hydronephrosis. Urol 2000; 56: 856.
15. Richard C. Case records of the Massachusetts General Hospital; weekly clinicopathological exercises; founded by Richard C. N Engl J Med 1954; 251: 396-400.
16. Bonekamp D, Horton KM, Hruban RH, *et al*. Castleman disease: the great mimic. Radiographics 2011; 31: 1793-807.
17. Enomoto K, Nakamichi I, Hamada K, *et al*. Unicentric and multicentric Castleman's disease. Br J Radiol 2007; 80: e24-6.
18. de Vries IA, van Acht MM, Demeyere TB. Neoadjuvant radiotherapy of primary irresectable unicentric Castleman's disease: a case report and review of the literature. Radiat Oncol 2010; 5: 7.
19. Chan JJ, Loh AH, Sim HG, *et al*. Coexistence of unicentric Castleman's disease and locally advanced papillary renal cell carcinoma: More than a coincidental association. Ann Acad Med Singapore 2010; 39: 584-92.
20. Takehara K, Sakai H, Igawa T, *et al*. Unicentric Castleman's disease with leiomyosarcoma: a rare association. Int J Urol 2003; 10: 619-21.
21. Venizelos I, Tamiolakis D, Simopoulos C, *et al*. Diffuse large B-cell lymphoma arising from a multicentric mixed variant of Castleman's disease. Indian J Cancer 2004; 41: 135-7.
22. Advani R, Warnke R, Rosenberg S, *et al*. Treatment of multicentric Castleman's disease complicated by development of non-Hodgkin's lymphoma with high-dose chemotherapy and autologous peripheral stem-cell support. Ann Oncol 1999; 10: 1207-9.
23. van Rhee F, Fayad L, Voorhees P, *et al*. Siltuximab, a novel anti-interleukin-6 monoclonal antibody for Castleman's disease. Respiratol 2010; 15: 1012-4.

卡斯托曼病在南臺灣一醫院之經驗

連啟惇 *,** 周世華 *** 吳俊杰 **** 黃明賢 **,***** 楊志仁 **,*****,******

卡斯托曼病是一種少見的淋巴增生性疾病且縱膈腔是最容易被侵犯的地方。因為少見所以它的病因及病理機轉仍然不明，起初的表現可以類似淋巴癌、單一惡性腫瘤、轉移癌或是感染症。依據卡斯托曼病獨特的淋巴結構可以區分為四種病理型態，包括單一中心型（透明血管變異及血漿細胞變異）、多重中心型、及人類皰疹病毒第八型相關的卡斯托曼病。卡斯托曼病的預後與分型有關，單一中心型通常有較好的預後，但是其還是可能會復發或合併其他種類卡斯托曼病與惡性腫瘤同時發生。我們從 1990 年起至 2010 年 5 月回顧高雄醫學大學附設醫院所有以病理確定診斷卡斯托曼病的病例，共計有 5 例。所有病例皆為單一中心型及透明血管變異。這些病例皆有良好預後，於手術切除診斷後追蹤至少一年以上皆無復發。我們發表這個研究整理及討論我們的發現。*(胸腔醫學 **2013; 28: 1-7**)*

關鍵詞：卡斯托曼病，單一中心型，透明血管型

高雄市立聯合醫院 內科部 *，高雄醫學大學附設中和紀念醫院 內科部 胸腔內科 **，外科部 胸腔外科 ***，病理部 ****，高雄醫學大學醫學院 內科系 *****，高雄市立大同醫院 內科部 ******
索取抽印本請聯絡：楊志仁醫師，高雄醫學大學附設中和紀念醫院 內科部 胸腔內科，高雄市十全一路 100 號

Efficacy Comparison of Conventional Computed Tomography and Whole-body ^{18}F-Fluorodeoxyglucose Positron Emission Tomography for Staging in Non-small Cell Lung Cancer Patients

Ping-Chih Hsu, Chih-Hung Chen, Kung-Chu Ho*, Yi-Chen Wu**, Kuo-Chin Kao***, Chien-Ying Liu, Wen-Cheng Chang****, Ying-Huang Tsai***, Cheng-Ta Yang***

Objectives: The prognosis of non-small cell lung cancer (NSCLC) is strongly correlated with the disease stage. Both ^{18}F-fluorodeoxyglucose positron emission tomography (FDG-PET) and conventional contrast-enhanced computed tomography (CT) are commonly used for staging, and their accuracies may thus influence the clinical outcome of NSCLC treatment. In this study, we investigated the efficacy of both methods for staging, particularly mediastinal nodal staging, in NSCLC patients.

Methods: From November 2006 to July 2010, 596 newly diagnosed NSCLC patients who had received chest CT and subsequent FDG-PET for initial staging were enrolled for assessment. Of these, 173 patients who received surgical resection without neoadjuvant therapy were further analyzed based on the final pathological stage.

Results: Compared to CT, FDG-PET led to upstaging in 180 (30.2%) patients and downstaging in 29 (4.9%). The pathological results of the 173 (31.0%) patients who received surgical intervention without neoadjuvant therapy revealed that the accuracy rate in staging was 57.8% by CT and 60.7% by PET. The sensitivity, specificity, positive predictive value, negative predictive value and accuracy for mediastinal nodal staging (N2) were 42.9%, 95.0%, 52.9%, 92.3% and 88.4% by CT, and 62.0%, 96.0%, 68.4%, 94.8% and 91.9% by PET, respectively.

Conclusions: This study suggests that FDG-PET is superior to conventional CT on the clinical staging of NSCLC, but there was still a false positive rate up to 31.6% in mediastinal staging or metastasis by FDG-PET. The false positive may cause that some patients receive inadequate treatment. Therefore, if nodal involvement is suspected by either image study which may alter the decision for surgical treatment, another invasive procedure may be required for tissue proof. ***(Thorac Med 2013; 28: 8-17)***

Key words: non-small cell lung cancer, ^{18}F-fluorodeoxyglucose positron emission tomography (FDG-PET), staging, mediastinal lymph node

Department of Thoracic Medicine, Chang Gung Memorial Hospital, Taoyuan, Taiwan; *Department of Nuclear Medicine and Molecular Imaging Center, Chang Gung Memorial Hospital, Taoyuan, Taiwan; **Department of Thoracic and Cardiovascular Surgery, Chang Gung Memorial Hospital, Taoyuan, Taiwan; ***Department of Respiratory Care, College of Medicine, Chang Gung University, Taoyuan, Taiwan; ****Department of Hematology–Oncology, Chang Gung Memorial Hospital, Taoyuan, Taiwan

Address reprint requests to: Dr. Cheng-Ta Yang, Department of Thoracic Medicine, Chang Gung Memorial Hospital, Taipei and Taoyuan, Taiwan, 199 Tun-Hwa North Road, Taipei 10507, Taiwan

Introduction

Lung cancer is a leading cause of cancer-related deaths in both males and females in Taiwan. Non-small cell lung cancer (NSCLC) accounts for most of the newly diagnosed cases of lung cancer each year [1]. The disease stage is strongly correlated with the prognosis and survival of NSCLC patients, and therefore appropriate initial staging of NSCLC is very important in decision-making with regard to treatment [2].

Fluorine-18 fluorodeoxyglucose positron emission tomography (FDG-PET) is commonly used for nodal staging and detecting distant metastasis in NSCLC patients, and for providing functional information on tumor metabolism [3]. FDG-PET is a non-invasive and sensitive tool, and its accuracy, in addition to findings on conventional contrast-enhanced computed tomography (CT), may substantially alter the treatment strategy for NSCLC patients [4].

Several studies have reported that FDG PET had an impact on the decision-making when planning treatment for NSCLC patients [5-7]. These studies reported that FDG-PET findings changed the initial stage in patients who were diagnosed with NSCLC, especially in cases of distant metastasis or advanced mediastinal lymph node involvement, and therefore futile thoracotomies were avoided. However, pulmonary inflammatory or granulomatous diseases such as organized pneumonia, tuberculosis (TB), or silicosis can cause an increased uptake signal in FDG-PET, resulting in an increase in false positive rates [8]. The matter of most concern in a TB-endemic area such as East Asia [9] is that such false positive results may lead to inadequate treatment for patients, and possibly even a lost opportunity for curative therapy. In this study, we investigated and compared the efficacy of FDG-PET and CT for staging, particularly mediastinal nodal staging, in Taiwanese patients with NSCLC. In addition, we evaluated whether the staging results of FDG-PET or CT were compatible with the final pathological results of the patients who received surgical treatment without neoadjuvant radiotherapy or chemotherapy.

Materials and Methods

Study subjects

We reviewed the medical records of NSCLC patients at Chang Gung Memorial Hospital, Linkou, Taoyuan, Taiwan between November 2006 and July 2010. The inclusion criteria were patients with newly diagnosed NSCLC proven by histology, and those who had received both chest CT and FDG-PET in the initial staging. A total of 596 patients were enrolled for analysis. The TNM staging system for NSCLC we used was that of the American Joint Committee on Cancer (AJCC) 6th edition.

Conventional staging procedures before FDG-PET

Before FDG-PET, the stage was determined by conventional staging procedures, which were performed depending on clinical needs. The conventional staging procedures included history, physical examination, chest radiography, enhanced chest and brain CT scans and bronchoscopy. In some cases, brain magnetic resonance imaging (MRI) was done because there were symptoms suggestive of metastasis, and enhanced brain CT did not provide a definite diagnosis. The results and data of all these conventional staging procedures were interpreted by experienced radiologists, as well as medical

oncologists or pulmonary physicians.

18F-FDG PET

Patients were intravenously injected with 370 MBq (10 mCi) of ^{18}F-FDG 1 hour before a whole body PET scan. They were instructed to fast for 6 hours before the examination. ^{18}F-FDG PET images were obtained using an ECAT EXACT HR+ camera (Siemens/CTI Inc., Knoxville, TN) using full width at half-maximum of 4.5 mm and a transaxial field of view of 15 cm. Transaxial, sagittal, and coronal scans were assessed primarily to detect the abnormal foci of increased FDG uptake. A visual analysis score (VAS) using a 4-point scale was primarily used to determine ^{18}FDG uptake in lymph nodes and other lesion sites, and the standardized uptake value was used as an accessory reference. The 4-point scale considered both the intensity of ^{18}F-FDG uptake in the lesion sites and the contrast between the background sites and lesion sites showing ^{18}F-FDG accumulation. A VAS of 3 or 4 was considered positive for malignancy, whereas a score of 1 or 2 was considered negative. An additional conventional non-contrast CT would be also done with the PET scan. The size and peripheral structure or organ direct invasion of the primary tumor were not evaluated by ^{18}F-FDG PET. This procedure was used mainly to detect lymph node involvement or distant metastasis. All of the images were interpreted by experienced nuclear physicians.

Comparison of CT and ^{18}F-FDG PET staging with pathological results

We reviewed the pathological stages of the patients who had received surgical resection without neoadjuvant therapy, and compared those findings with the CT and FDG-PET staging. Patients who had received radiotherapy and/or chemotherapy before surgery were excluded from this comparison.

Statistics

We calculated the sensitivity, specificity, positive (PPV) and negative predictive values (NPV) and accuracy for N2 involvement and distant metastasis as follows:

Sensitivity	true positive / true positive + false negative
Specificity	true negative / true negative + false positive
Positive predictive value (PPV)	true positive / all positive
Negative predictive value (NPV)	true negative / all negative
Accuracy	true positive + true negative / all cases

Results

Patient characteristics

In summary, there were 349 (58.6%) male and 247 (41.4%) female patients, with a median age of 66 years (range 30-90 years). The most predominant histological subtype of NSCLC was adenocarcinoma (n = 381, 63.9%), followed by squamous cell carcinoma (n = 143, 23.9%). Most patients had stage III disease (n = 193, 32.4%) before FDG-PET. The number of stage I and stage IV patients was similar (n = 161 [27%] and n = 163 [27.3%], respectively), and stage II patients accounted for the least proportion (n = 79, 13.3%) of patients in the study (Table 1).

Stage change after FDG-PET

In 65.0% of the patients, the stage before PET and after PET was concordant (Table 2).

Table 1. Characteristics of the 596 patients with non-small cell lung cancer

Characteristics	Number of patients (%)
Total patients	596
Gender	
Male	349 (58.6)
Female	247 (41.4)
Median age, years (range)	66 (30-90)
Pathology	
Adenocarcinoma	381 (63.9)
Squamous cell carcinoma	143 (23.9)
Non-small cell carcinoma	44 (7.4)
Bronchioloalveolar carcinoma	8 (1.3)
Other *	20 (3.4)
Stage before PET**	
Stage I	161 (27)
Stage II	79 (13.3)
Stage III	193 (32.4)
Stage IV	163 (27.3)
Patients received surgical resection without neoadjuvant therapy	173 (29.0)

* Large cell carcinoma, lymphoepithelial carcinoma, sarcomatoid carcinoma, or mixed type malignancy.

** Based on physical examination, chest radiation plain film, enhanced chest CT and enhanced brain CT, and brain MRI in some cases.

Ninety-two (38.8%) of the CT stage I and II patients were upstaged because of N2 and/or N3 lymph node involvement or distant metastasis after FDG-PET. Of 19 patients with distant metastasis detected by FDG-PET, 11 (58%) had bony metastasis only, 6 (31.6%) had lung-to-lung metastasis and pleural seeding, and 2 had distant lymph node involvement. The initial CT stage in 1 patient was T2aN0M0 stage IB; however, a hypermetabolic lesion was detected in the right axillary lymph node by FDG-PET. Nevertheless, the final pathology of this lymph node biopsy showed necrotizing granulation tissue, and the patient finally underwent curative surgery for the primary lung tumor.

Seventy (36.2%) CT stage III patients were upstaged to stage IV because metastasis was detected, and 4 (2%) patients were downstaged. Bone metastasis was detected in 99 patients using FDG-PET, and was the most extrathoracic distant metastatic site that was detected by this method. Forty-six of the 99 patients had bone metastasis that was not detected in conventional CT, and they were subsequently upstaged to stage IV. In addition, liver cancer was detected in 4 patients by FDG-PET, but liver metastasis was not found on conventional CT initially. The brain metastasis of 19 patients was detected by conventional contrast-enhanced brain CT or brain MRI initially. Nineteen (11.7%) of the CT stage IV patients were downstaged. Twelve of these 19 patients were diagnosed with lung-to-lung metastasis by chest CT initially, but these nodules did not present as hypermetabolism on FDG-PET. Overall, 180 (30.2%) patients were upstaged and 29 (4.9%) were downstaged after FDG-PET.

Accuracy of CT and FDG-PET for staging based on the pathological findings

The pathological findings of 100 (57.8%) and 105 (60.7%) cases were in agreement with CT and FDG-PET staging, respectively (Table 3 and Table 4). The sensitivity, specificity, PPV, NPV and accuracy for N2 involvement and metastasis by CT or FDG-PET staging were calculated based on the pathological diagnoses (Table 5 and Table 6). The sensitivity and PPV of both CT and FDG-PET were somewhat low. The sensitivity and PPV for CT were 42.90% and 52.90%, respectively, and for FDG-PET,

Table 2. Comparison of the stage of NSCLC before and after PET in the 596 patient

Stage before PET		Number of patients	Satge after PET (number of patients)							Upstaging (%)	Down staging (%)
			IA	IB	IIA	IIB	IIIA	IIIB	IV		
I	IA	79	57	0	7	1	5	5	4	22	0
	IB	82	0	53	5	1	17	5	1	29	0
II	IIA	43	3	3	16	0	8	7	6	21	6
	IIB	36	0	0	0	16	11	1	8	20	0
III	IIIA	94	0	0	0	1	42	18	33	51	1
	IIIB	99	0	0	0	0	3	59	37	37	3
IV	IV	163	1	3	1	2	4	8	144	0	19
	Total	596								180 (30.2)	29 (4.9)

Table 3. Comparison of CT and pathological stages of patients who received surgical resection without neoadjuvant therapy

CT stage		Total	Pathology stage (number of patients)							Accurate rate (%)
			IA	IB	IIA	IIB	IIIA	IIIB	IV	
I	IA	62	36	14	8	0	3	0	1	36
	IB	47	0	37	7	0	3	0	0	37
II	IIA	25	7	0	14	2	2	0	0	14
	IIB	18	0	0	4	5	9	1	0	5
III	IIIA	14	1	3	0	1	8	1	0	8
	IIIB	0	0	0	0	0	0	0	0	0
	IV	7	0	4	0	1	2	0	0	0
	Total	173								100 (57.8)

61.90% and 68.40%, respectively. Both CT and FDG-PET had higher specificity rates, NPVs and accuracy. The specificity rate, NPV and accuracy for CT were 95.0%, 92.30%, and 88.40%, respectively, and 96.0%, 94.80% and 91.90%, respectively, for FDG-PET.

In 8 patients, conventional CT initially found mediastinal lymph nodes that were determined to be malignant. However, 1 of these 8 patients had hamartoma, 1 had bronchopneumoniae and the other 6 had only fibrosis lesions, which were found finally by pathologic examinations. Of the 12 patients whose mediastinal nodes were diagnosed finally as malignant on the pathologic examinations, all were smaller than 1 cm in diameter on CT examination.

Mediastinal lymph nodes in 6 patients showed a hypermetabolic signal on FDG-PET, and were proposed to be malignant metastasis initially, but on the final pathology, 4 of them were diagnosed as reactive nodes, 1 was caseous necrotizing granuloma and the other was silicosis. Eight patients who were diagnosed as having mediastinal lymph node metastasis on

Table 4. Comparison of ^{18}F-FDG PET and pathological stages of patients who received surgical resection without neoadjuvant therap

PET stage		Total	Pathology stage (number of patients)							Accurate rate (%)
			IA	IB	IIA	IIB	IIIA	IIIB	IV	
I	IA	54	36	11	5	0	1	0	1	36
	IB	48	5	34	5	1	3	0	0	34
II	IIA	24	2	4	15	0	3	0	0	15
	IIB	19	0	2	6	5	5	1	0	5
III	IIIA	27	1	5	3	2	15	1	0	15
	IIIB	0	0	0	0	0	0	0	0	0
IV	IV	1	0	1	0	0	0	0	0	0
	Total	173	44	57	34	8	27	2	1	105 (60.7)

Table 5. Contingency table for CT and FDG-PET staging in N2 involvement

	Pathology N2 positive	Pathology N2 negative
CT N2 positive	9	8
CT N2 negative	12	144
PET N2 positive	13	6
PET N2 negative	8	146

Table 6. Sensitivity, specificity, positive predictive value (PPV), negative predictive value (NPV), and accuracy of CT and PET for N2 involvement and distant metastasis

	CT	PET
Sensitivity	42.90%	61.9%
Specificity	95.0%	96.0%
Positive predictive value (PPV)	52.90%	68.40%
Negative predictive value (NPV)	92.30%	94.80%
Accuracy	88.40%	91.90%

the final pathologic examination had a weak signal on FDG-PET initially, and the standardized uptake values (SUV) were all less than 2.

Discussion

Whole body PET is a useful and less invasive procedure to improve staging for head and neck cancer, lymphoma, soft tissue sarcoma, gastrointestinal stromal tumors and lung cancer. However, the role of FDG-PET in NSCLC is still unclear. In the present study, the initial staging was changed after FDG-PET in 209 (35.0%) patients, including 180 (30.2%) who were upstaged and 29 (4.9%) who were downstaged. This is similar to results in previous

retrospective and prospective studies [10-11]. Margery *et al*. reported that FDG-PET changed the initial stage in approximately 29% of patients with NSCLC [11]. Another large retrospective study found that the initial staging of 29.6% of NSCLC patients was altered because of FDG-PET findings [10].

Detection of N2 and/or N3 involvement is a crucial issue in determining the needs for neoadjuvant therapy in surgical candidates [12]. The sensitivity of FDG-PET for mediastinal node detection has been reported to be 40% to 91.6% in several studies [13-15]. All the specificities were higher than 80% in these studies, and the PPV was around 70% with the NPV ranging from 83% to 98% [13-16]. In our study, the sensitivity and PPV of FDG-PET for mediastinal node metastasis were 61.90% and 68.40%, respectively, which were higher than those of CT (42.90% and 52.90%, respectively). Higher specificity, NPV and accuracy of FDG-PET (more than 90% for all 3) were also shown in the present study. Based on the high specificity and NPV of FDG-PET in this study, we suggest that FDG-PET is a more accurate tool than CT for staging of NSCLC patients, and in particular those who have potentially resectable disease.

However, FDG-PET had a false positive rate of up to 31.6% in mediastinal staging, and the sensitivity was only 61.90% in the present study. We reviewed the pathology of the 6 patients who had a false positive for N2 metastasis on FDG-PET, and found that the mediastinal lymph nodes of 4 patients were reactive nodes, another was a proven caseous necrotizing granuloma and the other was silicosis. As is well known, abnormal FDG uptake frequently occurs in granulomatous or inflammatory diseases [17-18]. In TB-endemic areas such as East Asia, including Taiwan [9,16]. FDG-PET has been reported to have a relatively low sensitivity and PPV in nodal staging of NSCLC. A previous study in another TB-endemic area also showed a sensitivity of only 61% for FDG-PET in mediastinal lymph node detection, which is similar to our result [19]. The patients in this study were all residents of Taiwan, where the prevalence of TB infection is much higher than in Western countries [9,16].

Although FDG-PET may prevent some unnecessary surgical procedures, most clinicians are also concerned about the high false positive rate in mediastinal node and metastasis staging, which may mistakenly change curative treatment to palliative care. There have been some improvements in measurement techniques in FDG-PET for nodal staging; however, the diagnostic accuracy of FDG-PET has not improved much as a result [16,20]. Although Tournoy *et al*. proposed alternative SUV parameters such as the node/liver SUV ratio, which could have better sensitivity and specificity than lymph node SUV for diagnosis of N2 disease, this study finally concluded that invasive intrathoracic lymph node staging may not be replaced by FDG PET [21]. Therefore, if there is suspected mediastinal nodal involvement on either CT or FDG-PET, further invasive procedures such as endobronchial ultrasound-guided transbronchial aspiration or mediastinoscopy for direct tissue proof may be required for adequate diagnosis and staging [22-24].

In conclusion, FDG-PET provides more accurate and efficient staging than conventional enhanced CT for NSCLC patients, especially for those who have potentially resectable disease. However, for mediastinal nodal involvement and distant metastasis patients, further invasive procedures may sometimes be needed

for direct tissue proof, especially in TB-endemic areas.

References

1. Alberg AJ, Samet JM. Epidemiology of lung cancer. Chest 2003; 123(1 Suppl): 21S-49S.
2. Fukui T, Mori S, Hatooka S, *et al*. Prognostic evaluation based on a new TNM staging system proposed by the International Association for the Study of Lung Cancer for resected non-small cell lung cancers. J Thorac Cardiovasc Surg 2008; 136(5): 1343-8.
3. Kuo CH, Chen HC, Chung FT, *et al*. Diagnostic value of EBUS-TBNA for lung cancer with non-enlarged lymph nodes: a study in a tuberculosis-endemic country. PLoS One 2011; 6(2): e16877.
4. Pieterman RM, van Putten JW, Meuzelaar JJ, *et al*. Preoperative staging of non-small-cell lung cancer with positron-emission tomography. N Engl J Med 2000; 343(4): 254-61.
5. Sachs S, Bilfinger TV. The impact of positron emission tomography on clinical decision making in a university-based multidisciplinary lung cancer practice. Chest 2005; 128(2): 698-703.
6. Heresi GA, Mazzone PJ, Stoller JK. Impact of positron emission tomography on clinical decision making. Chest 2006; 130(1): 300-1.
7. Fischer B, Lassen U, Mortensen J, *et al*. Preoperative staging of lung cancer with combined PET-CT. N Engl J Med 2009; 361(1): 32-9.
8. Asad S, Aquino SL, Piyavisetpat N, *et al*. False-positive FDG positron emission tomography uptake in nonmalignant chest abnormalities. AJR Am J Roentgenol 2004; 182(4): 983-9.
9. Chiu YS, Wang JT, Chang SC, *et al*. Mycobacterium tuberculosis bacteremia in HIV-negative patients. J Formos Med Assoc 2007; 106(5): 355-64.
10. Heo EY, Yang SC, Yoo CG, *et al*. Impact of whole-body (1)F-fluorodeoxyglucose positron emission tomography on therapeutic management of non-small cell lung cancer. Respirology 2010; 15(8): 1174-8.
11. Margery J, Milleron B, Vaylet F, *et al*. [Impact of positron emission tomography on clinical management of potentially resectable non-small-cell lung cancer: a French prospective multicenter study]. Rev Pneumol Clin 2010; 66(5): 313-20.
12. Muehling B, Wehrmann C, Oberhuber A, *et al*. Comparison of clinical and surgical-pathological staging in IIIA non-small cell lung cancer patients. Ann Surg Oncol 2011.
13. Lv YL, Yuan DM, Wang K, *et al*. Diagnostic performance of integrated positron emission tomography/computed tomography for mediastinal lymph node staging in non-small cell lung cancer: A bivariate systematic review and meta-analysis. J Thorac Oncol 2011; 6(8): 1350-8.
14. Konishi J, Yamazaki K, Tsukamoto E, *et al*. Mediastinal lymph node staging by FDG-PET in patients with non-small cell lung cancer: analysis of false-positive FDG-PET findings. Respiration 2003; 70(5): 500-6.
15. Schrevens L, Lorent N, Dooms C, *et al*. The role of PET scan in diagnosis, staging, and management of non-small cell lung cancer. Oncologist 2004; 9(6): 633-43.
16. Yen RF, Chen KC, Lee JM, *et al*. 18F-FDG PET for the lymph node staging of non-small cell lung cancer in a tuberculosis-endemic country: is dual time point imaging worth the effort? Eur J Nucl Med Mol Imaging 2008; 35(7): 1305-15.
17. Bakheet SM, Powe J. Benign causes of 18-FDG uptake on whole body imaging. Semin Nucl Med 1998; 28(4): 352-8.
18. Roberts PF, Follette DM, von Haag D, *et al*. Factors associated with false-positive staging of lung cancer by positron emission tomography. Ann Thorac Surg 2000; 70(4): 1154-9.
19. Kim YK, Lee KS, Kim BT, *et al*. Mediastinal nodal staging of non-small cell lung cancer using integrated 18F-FDG PET/CT in a tuberculosis-endemic country: diagnostic efficacy in 674 patients. Cancer 2007; 109(6): 1068-77.
20. Kasai T, Motoori K, Horikoshi T, *et al*. Dual-time point scanning of integrated FDG PET/CT for the evaluation of mediastinal and hilar lymph nodes in non-small cell lung cancer diagnosed as operable by contrast-enhanced CT. Eur J Radiol 2010; 75(2): 143-6.
21. Tournoy KG, Maddens S, Gosselin R, *et al*. Integrated FDG-PET/CT does not make invasive staging of the intrathoracic lymph nodes in non-small cell lung cancer redundant: a prospective study. Thorax 2007; 62(8): 696-701.
22. Turkmen C, Sonmezoglu K, Toker A, *et al*. The additional

value of FDG PET imaging for distinguishing N0 or N1 from N2 stage in preoperative staging of non-small cell lung cancer in region where the prevalence of inflammatory lung disease is high. Clin Nucl Med 2007; 32(8): 607-12.

23. Metin M, Citak N, Sayar A, *et al*. The role of extended cervical mediastinoscopy in staging of non-small cell lung cancer of the left lung and a comparison with integrated positron emission tomography and computed tomography: Does integrated positron emission tomography and computed tomography reduce the need for invasive procedures? J Thorac Oncol 2011 Oct; 6(10): 1713-9.
24. Cetinkaya E, Seyhan EC, Ozgul A, *et al*. Efficacy of convex probe endobronchial ultrasound (CP-EBUS) assisted transbronchial needle aspiration for mediastinal staging in non-small cell lung cancer cases with mediastinal lymphadenopathy. Ann Thorac Cardiovasc Surg 2011; 17(3): 236-42.

傳統電腦斷層和正子掃瞄在非小細胞癌診斷分期上的準確度分析比較

徐稟智　陳志弘　何恭之 *　吳怡成 **　高國晉 ***　劉劍英　張文震 ****
蔡熒煌 ***　楊政達 ***

背景：非小細胞肺癌（non-small cell lung cancer, NSCLC）的分期和預後有重要的關連，正子掃瞄（^{18}F-fluorodeoxyglucose positron emission tomography, FDG PET）和傳統電腦斷層掃瞄已經普遍使用在非小細胞肺癌的診斷和分期上。然而這兩項檢查的準確度可能影響在臨床上的治療計畫，尤其是在縱膈腔淋巴結（N2）診斷方面。所以本研究目的在於分析這兩項檢查在非小細胞肺癌的分期準確度比較。

方法：本研究瀏覽了自 2006 年 11 月到 2010 年 7 月，596 名新診斷的非小細胞肺癌的病患，並且在初診斷時同接受正子掃瞄和傳統電腦斷層掃瞄者，分析其分期治療計畫的改變。在接受手術的病患中，以最後病理確定的診斷分期去比較這兩者檢查在分期上的準確度。

結果：相較於傳統電腦斷層，加上全身正子掃瞄之後，有百分之三十的病人分期上的改變是上升的，另外百分之四點九的病人分期下降，因此，百分之二十六點三的病人會改變原本的治療計畫。其中有一百七十三名病人在沒有接受任何前置輔助治療（Neoadjuvant therapy）下直接接受手術治療，以這些手術後的病理組織作為最後分期診斷的根據比較，電腦斷層的準確率為百分之五十七點八，全身正子掃瞄為百分之六十點七。對於縱膈腔淋巴結（N2）分期的診斷靈敏度（Sensitivity）、特異度（Specificity）、陽性預測值（Positive predictive value）、陰性預測值（Negative predictive value）和準確率（Accuracy），在電腦斷層分別為 42.9%, 95.0%, 52.9%, 92.3% 及 88.4%，而在正子掃瞄方面為 62.0%, 96.0%, 68.4%, 94.8% 及 91.9%。

結論：該研究顯示出正子掃瞄（FDG PET）對於非小細胞肺癌的臨床分期上是稍優於電腦斷層。但是在在縱膈腔淋巴結（N2）或遠處轉移分期診斷方面仍有三成左右的偽陽性率，這也可能使得有些病人失去痊癒治療的機會。因此，當這兩項檢查有懷疑癌細胞縱膈腔淋巴結侵犯時，或許進一步侵襲性的如經內視鏡超音波穿刺或縱膈腔鏡去直接取得組織證實是建議必要的。*(胸腔醫學* ***2013; 28: 8-17)***

關鍵詞：非小細胞肺癌，正子掃瞄，分期，縱膈腔淋巴結

長庚醫療財團法人林口長庚紀念醫院　呼吸胸腔內科系，* 長庚醫療財團法人林口長庚紀念醫院　核子醫學科
** 長庚醫療財團法人林口長庚紀念醫院　心臟暨胸腔外科，*** 長庚大學　呼吸照護學系
**** 長庚醫療財團法人林口長庚紀念醫院　血液腫瘤科
索取抽印本請聯絡：楊政達醫師，長庚醫療財團法人林口長庚紀念醫院　呼吸胸腔內科系，台北市 10507 敦化北路 199 號

Pulmonary Alveolar Proteinosis Combined with Pulmonary Aspergillosis in an Elderly Patient: A Case Report and Literature Review

Ping-Hsien Tsou, Pin-Kuei Fu, Yi-Hsien Chen*, Gwan-Han Shen, Jeng-Yuan Hsu

Pulmonary alveolar proteinosis (PAP) is a rare disease characterized by the accumulation of surfactant lipids and proteins in the alveoli of the lungs, leading to respiratory insufficiency and alveolar macrophage dysfunction. The median age at diagnosis is 42 years. It is uncommon in the elderly and has a high morbidity, mainly from respiratory failure and infection. We report the case of a 74-year-old female diabetic patient with PAP and pulmonary aspergillosis complicated by severe hypoxemic respiratory failure and long-term ventilator dependence. The hypoxemia was resolved, lung infiltrates reduced, and the patient was weaned from the ventilator after successful anti-fungal therapy and sequential unilateral whole lung lavage. ***(Thorac Med 2013; 28: 18-24)***

Key words: pulmonary alveolar proteinosis, aspergillosis, long-term ventilator dependence

Introduction

Pulmonary alveolar proteinosis (PAP) is a rare syndrome that is characterized by the accumulation of surfactant lipids and proteins in the alveoli and terminal airways, causing respiratory insufficiency. A systematic review of 241 PAP cases in China found that the median age at diagnosis was 42 years, ranging from 40 days to 66 years [1]. High levels of granulocyte-macrophage colony-stimulating factor (GM-CSF), which neutralizes auto-antibodies, are detected specifically in patients with idiopathic PAP [2]. In GM-CSF gene knockout PAP mice, mortality from infection and susceptibility to bacterial, fungal, and mycobacterial pathogens were increased [3]. Thus, it has long been recognized that patients with PAP are at risk of secondary infections with a variety of organisms, leading to pulmonary, systemic and disseminated diseases [4].

In 1993, Kita *et al* [5] reported the autopsy finding from a 49-year-old woman with acute lymphocytic leukemia (ALL) associated with secondary PAP and systemic aspergillosis. In 2002, Katagiri [6] *et al* reported the case of a 53-year-old woman with acute myeloid leukemia (AML) with pulmonary aspergillosis and

Department of Internal Medicine, Division of Chest Medicine, Taichung Veterans General Hospital, Taichung, Taiwan; *Department of Pathology, Taichung Veterans General Hospital, Taichung, Taiwan
Address reprint requests to: Dr. Gwan-Han Shen, Department of Internal Medicine, Division of Chest Medicine, Taichung Veterans General Hospital, 160, Sec. 3, Taichung Port Road, Taichung 40705, Taiwan

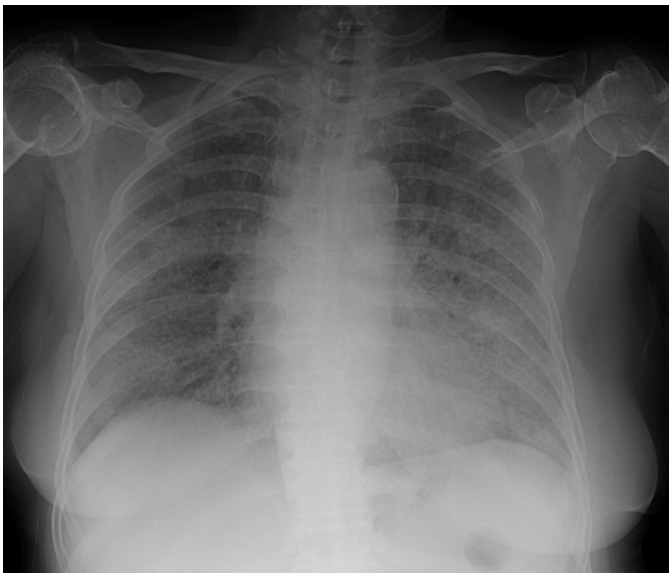

(A)

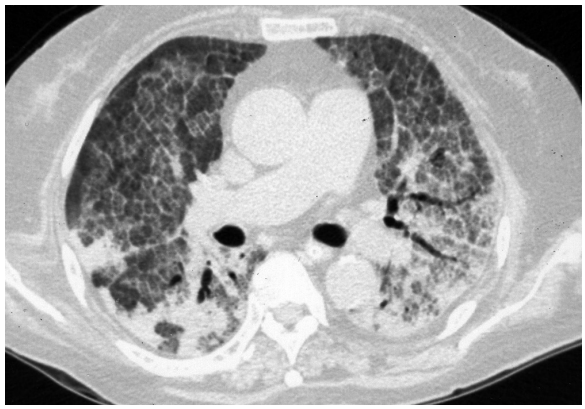

(B)

Fig. 1. (A) Chest X-ray shows bilateral, diffuse alveolar infiltrations. (B) Chest HRCT shows diffuse ground-glass opacity and inter-lobular septal thickening, resulting in a crazy-paving pattern and consolidation of the bilateral lower lobes.

secondary PAP. In 2010, Lin [7] *et al* reported the case of a 71-year-old woman with rhinocerebral aspergillosis and secondary PAP, successfully treated by anti-fungal therapy. However, secondary PAP associated with pulmonary aspergillosis in a patient with no hematological malignancy has not been reported before. We herein report a 74-year-old woman with rare old-age-onset PAP associated with pulmonary aspergillosis, successfully treated with whole lung lavage and anti-fungal therapy.

Case Report

A 74-year-old woman was transferred from a local hospital due to progressive dyspnea and productive cough. Five months previous to this, she began to have dyspnea on exertion that gradually increased in severity, and she became bedridden. She also had productive cough with jelly-like sputum, but had no fever, chills, or hemoptysis. She had been repeatedly hospitalized and treated for bacterial pneumonia and congestive heart failure with antibiotics and diuretics, but in vain. She was a non-smoker, and had had hypertension and diabetes mellitus for 18 years under treatment with oral hypoglycemic drugs.

On admission at the emergency department, she had dyspnea and cyanosis. Her temperature was 37.8°C, pulse rate 104, respiratory rate 20 per minute, blood pressure 114/63 mmHg, and oxygen saturation 87% in room air. Chest examination disclosed fine crackles in both lungs. Arterial blood gas analysis while the patient was breathing ambient air revealed a pH of 7.52, PaO_2 48.7 mmHg, $PaCO_2$ 48.3 mmHg, and bicarbonate 39.2 mmol/L. Hemogram and blood biochemistry studies revealed leukocytosis (WBC 18600/cumm), elevated C-reactive protein (hs-CRP 1.21 mg/dL; reference range <0.3 mg/dL), hyperglycemia (glucose 413 mg/dL) and an elevated lactate dehydrogenase level (LDH, 557 U/l; normal range, 120-240 U/l). The serum creatinine level was 1.0 mg/dL.

Electrocardiogram revealed sinus tachycardia, and chest radiograph revealed bilateral,

diffuse alveolar infiltration without pleural effusion (Figure 1A). She was intubated and mechanically ventilated for hypoxemic and hypercapnic respiratory failure. High-resolution computed tomography (HRCT) of the chest revealed diffuse ground-glass opacity and interlobular septal thickening resulting in a crazy-paving pattern, and consolidation of the bilateral lower lobes (Figure 1B). PAP or non-specific interstitial pneumonitis was the initial differential diagnosis.

She was given empirical antimicrobial therapy with ampicillin/sulbactam at the emergency department, and was admitted to the respiratory intensive care unit (ICU). During the next 24 hours, her blood pressure went down to 86/54 mmHg, with leukocytosis, pyuria, and purulent sputum. Intravenous fluids and piperacillin/tazobactam were administered, and improved her blood pressure. Urine, blood, and sputum specimens were sent for culture. Broncho-alveolar lavage (BAL) fluid returned from the right middle lung had a milky appearance. Cytological examination of the BAL fluid showed many periodic acid-Schiff (PAS)-positive granular eosinophilic materials (Figure 2A). Papanicolaou staining of the BAL fluid showed abundant pauci-cellular pale granular materials, and round or oval globules with an orange-colored center and green rim (Figure 2B), which were compatible with PAP. Moreover, BAL fluid culture and endotracheal aspiration grew *Aspergillus fumigatus*, and urine culture grew *Escherichia coli*. Blood culture was negative.

Systemic anti-fungal therapy with oral itraconazole (200 mg every 12 h) was administered. However, the patient's respiratory status continued to deteriorate after BAL. She was sedated and paralyzed, with ventilation settings configured at a pressure-regulated volume control of 380 ml, 65-90% oxygen, positive end-expiratory pressure (PEEP) of 14 cm H_2O, and respiratory rate of 24 breaths per minute. The bilateral diffuse alveolar opacities on chest X-ray improved after 1 week of oral itraconazole therapy. To avoid worsening of the Aspergillus infection, whole lung lavage was performed after 1 week of anti-fungal therapy.

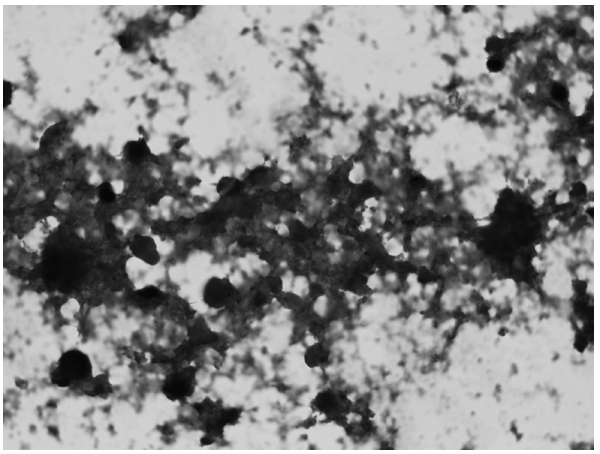

(A)

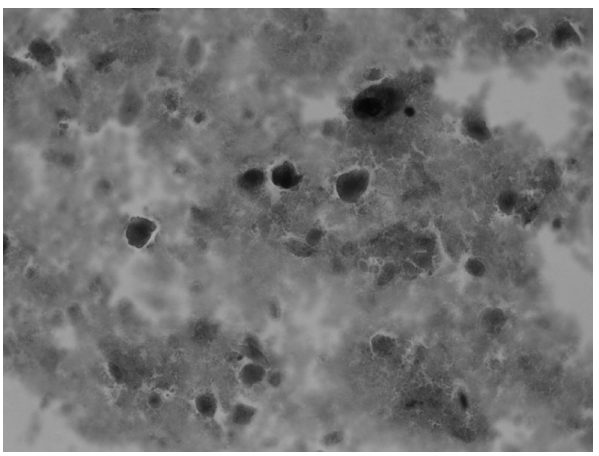

(B)

Fig. 2. (A) Cytology smear of BAL fluid shows amorphous materials that are PAS-positive (1000X). (B) Cytology smear of BAL fluid shows globules stained green at the rim and orange in the center (Papanicolaou stain, 1000X).

To check if the patient could tolerate single-

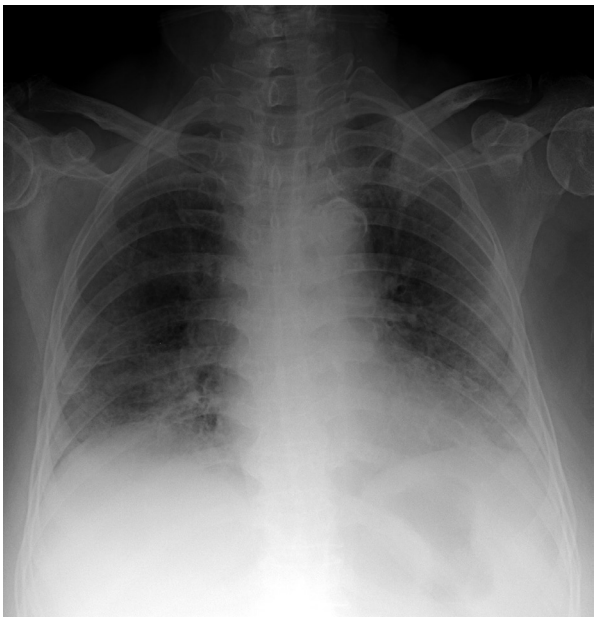

Fig. 3. Chest X-ray showed partial clearance of bilateral lung infiltrates.

lung ventilation, we replaced the single-lumen endotracheal tube with a double-lumen tube at the respiratory ICU, and each lung was ventilated independently for 1 hour prior to whole lung lavage. The left lung was lavaged first, while the right lung was independently ventilated. A total of 5.5 L of saline were instilled in 10 exchanges, and 5 L returned from the left lung, requiring 65 min to complete. Milky fluid that was obtained from the lavage became progressively less opaque. The procedure was stopped because the oxygen saturation had dropped to <80%.

After the incomplete unilateral whole lung lavage, the patient returned to the respiratory ICU with a single-lumen endotracheal tube. Initial PaO_2 was 65 mmHg on FiO_2 of 1.0. Due to the severe hypoxemia during left lung lavage, right lung lavage was postponed. The patient was ventilator-dependent for the next 45 days and underwent 5 weeks of anti-fungal therapy. Before the sequential right lung lavage, PaO_2 had already increased to 70 mmHg on FiO_2 of 0.4. She then received sequential right lung lavage with 5 L of saline. She was successfully weaned from the ventilator 5 days after the right lung lavage.

A chest radiograph revealed reduced bilateral lung infiltrates (Figure 3). She was discharged within 1 week, and received home oxygen at 3 L/min by nasal cannula. On follow-up at the outpatient clinic 1 month later, her dyspnea had markedly improved, with exercise tolerance near baseline. Anti-fungal therapy was continued until chest radiographic abnormalities had resolved.

Discussion

PAP usually presents with progressive dyspnea of gradual onset, and may be associated with low-grade fever [8]. Marked fever usually indicates the presence of a complicating pulmonary infection. Biochemical abnormalities may include elevated serum levels of LDH [9]. In the HRCT scan, PAP has a characteristic appearance of patchy or geographic air-space "ground-glass" opacities or consolidation, with thickening of the inter-lobular septa, resulting in a "crazy-paving" pattern [10]. An acceptable PAP diagnosis is based on histopathologic findings of specimens obtained by open lung biopsy, transbronchial lung biopsy (TBLB), video-assisted thoracoscopic surgery (VATS) biopsy or on cytologic findings in BAL fluid samples [11]. In the past, the diagnosis of PAP required open-lung biopsy, which remains the "gold standard" [4]. Open-lung biopsy is less commonly required now, because diagnosis can be established in clinically suspected cases by a typical CT-scan presentation, the clas-

sic findings of a "milky" appearance, and the characteristic cytology findings of BAL fluid [12]. The cytology of BAL fluid often shows large amounts of granular eosinophilic material with morphologically abnormal "foamy" macrophages engorged with PAS-positive intracellular inclusions [4]. PAS is not routinely performed for all BAL fluid specimens because a diagnosis of PAP is not usually expected. The routinely performed staining method, Papanicolaou staining, which often reveals the presence of round or oval "globules" with an orange-colored center and green rim, has proved to be useful in aiding the diagnosis, especially when the number of globules is more than 18 [13].

PAP is further subdivided into congenital, idiopathic, and secondary categories, depending on whether it is caused by several genetic diseases borne by mutations in GM-CSF receptor α chain (CSF2RA) or GM-CSF receptor β chain (CSFR2B) genes [14] or a primary disturbance of GM-CSF signaling [8], or is secondary to another disease, such as hematologic disorders, malignancy, immune deficiency syndromes, chronic inflammatory disorders, and chronic infections [15]. There are a few reports of Aspergillus infections associated with PAP, and these were mainly pulmonary [16] or invasive rhino-cerebral aspergillosis [7], except 1 case of systemic aspergillosis defined at autopsy [5]. Most reported cases with concomitant PAP and aspergillosis in the literature are of patients with hematologic malignancies [7].

The mechanisms of secondary PAP associated with infection are less clear [8]. Most of these infections are confined to the lungs. The infection may lead to alveolar macrophage dysfunction and impaired pulmonary clearance of surfactant, which by nature is a good culture medium [4].

Secondary PAP, in some cases caused by extra-pulmonary aspergillosis, can be resolved by eradicating the underlying extra-pulmonary infection [7]. Non-resolving secondary PAP can be effectively treated by whole-lung lavage, although this has not been well studied [8].

In the present case, pulmonary aspergillosis was not initially detected until the BAL fluid cytology revealed PAP and culture revealed co-existing pulmonary aspergillosis. Hematologic malignancy and rhino-cerebral aspergillosis were excluded by the absence of both abnormal blood cells and clinical manifestations of sinusitis, like purulent nasal discharge, facial tenderness, headache, and nasal obstruction.

Elderly patients without hematologic malignancy and with secondary PAP, pulmonary aspergillosis and chronic ventilator-dependent respiratory failure are rare, since PAP is uncommon in the elderly [1] and PAP patients, rarely require long-term mechanical ventilation [17]. Our patient could have been weaned earlier from long-term ventilation if the right lung had been lavaged earlier. The issue of delayed right lung lavage can be viewed in 2 ways. First, the profound hypoxemia that occurs during lavage could be life-threatening. Second, after anti-fungal therapy, the patient's oxygenation improved gradually. The delay allowed the subsequent right lung lavage to be performed more safely, and avoided any life-threatening hypoxemia.

This case demonstrates the importance of detecting concomitant infectious disease in a patient with PAP. Early anti-microbial therapy is as important as successful whole lung lavage.

References

1. Xu Z, Jing J, Wang H, *et al*. Pulmonary alveolar proteinosis in China: a systematic review of 241 cases. Respiro-

logy 2009; 14: 761-6.
2. Suzuki T, Sakagami T, Young LR, *et al*. Hereditary pulmonary alveolar proteinosis: pathogenesis, presentation, diagnosis, and therapy. American journal of respiratory and critical care medicine 2010; 182: 1292-304.
3. Uchida K, Beck DC, Yamamoto T, *et al*. GM-CSF autoantibodies and neutrophil dysfunction in pulmonary alveolar proteinosis. The New England journal of medicine 2007; 356: 567-79.
4. Seymour JF,Presneill JJ. Pulmonary alveolar proteinosis: progress in the first 44 years. American journal of respiratory and critical care medicine 2002; 166: 215-35.
5. Kita H, Muro S, Nakano Y, *et al*. [An autopsy case of acute lymphocytic leukemia associated with secondary pulmonary alveolar proteinosis and systemic aspergillosis]. Nihon Kyobu Shikkan Gakkai Zasshi 1993; 31: 374-8.
6. Katagiri T, Shimamoto T, Shoji N, *et al*. [Invasive aspergillosis and pulmonary alveolar proteinosis in acute myeloid leukemia]. [Rinsho ketsueki] The Japanese journal of clinical hematology 2002; 43: 871-4.
7. Lin KP, Sheng WH, Wang CP, *et al*. Resolution of secondary pulmonary alveolar proteinosis following treatment of rhinocerebral aspergillosis. International journal of infectious diseases: IJID: official publication of the International Society for Infectious Diseases 2010; 14 Suppl 3: e246-9.
8. Murray JF, Mason RJ, Murray and Nadel's textbook of respiratory medicine. 5th ed. 2010, Philadelphia, PA: Saunders/Elsevier.
9. Lin FC, Chen YC, Chang SC. Clinical importance of bronchoalveolar lavage fluid and blood cytokines, surfactant protein D, and Kerbs von Lungren 6 antigen in idiopathic pulmonary alveolar proteinosis. Mayo Clinic proceedings. Mayo Clinic 2008; 83: 1344-9.
10. Holbert JM, Costello P, Li W, *et al*. CT features of pulmonary alveolar proteinosis. AJR. American journal of roentgenology 2001; 176: 1287-94.
11. Inoue Y, Trapnell BC, Tazawa R, *et al*. Characteristics of a large cohort of patients with autoimmune pulmonary alveolar proteinosis in Japan. American journal of respiratory and critical care medicine 2008; 177: 752-62.
12. Delaval P, Brinchault G, Corre R, *et al*. [Pulmonary alveolar phospholipoproteinosis]. Revue de pneumologie clinique 2005; 61: 186-92.
13. Chou CW, Lin FC, Tung SM, *et al*. Diagnosis of pulmonary alveolar proteinosis: usefulness of papanicolaou-stained smears of bronchoalveolar lavage fluid. Archives of internal medicine 2001; 161: 562-6.
14. Dirksen U, Nishinakamura R, Groneck P, *et al*. Human pulmonary alveolar proteinosis associated with a defect in GM-CSF/IL-3/IL-5 receptor common beta chain expression. The Journal of clinical investigation 1997; 100: 2211-7.
15. Borie R, Danel C, Debray MP, *et al*. Pulmonary alveolar proteinosis. European respiratory review: an official journal of the European Respiratory Society 2011; 20: 98-107.
16. Kobayashi T, Ebina M, Oshima M, *et al*. [Case of alveolar proteinosis associated with pulmonary aspergillosis]. Nihon Naika Gakkai zasshi. The Journal of the Japanese Society of Internal Medicine 1999; 88: 135-7.
17. Cohen ES, Elpern E, Silver MR. Pulmonary alveolar proteinosis causing severe hypoxemic respiratory failure treated with sequential whole-lung lavage utilizing venovenous extracorporeal membrane oxygenation: a case report and review. Chest 2001; 120: 1024-6.

老年病人肺泡蛋白沉積症合併肺麴菌感染：病例報告與文獻回顧

鄒秉誠　傅彬貴　陳奕先 *　沈光漢　許正園

肺泡蛋白沉積症是一種罕見的疾病。此疾病與肺表面活性劑在肺部累積，肺泡巨噬細胞失能有關，導致呼吸困難與肺部免疫機能缺失。此疾病診斷的平均年齡為 42 歲，老年人的肺泡蛋白沉積症並不常見。老年人常見的併發症包括嚴重呼吸衰竭與繼發機會性感染。我們報告一個 74 歲的肺泡蛋白沉積症病人，合併嚴重低血氧呼吸衰竭與肺麴菌感染。病人在抗麴菌治療後，接受了單側循序性的全肺灌洗，成功的治療了呼吸衰竭，並脫離了長時間依賴的呼吸器。*(胸腔醫學 **2013; 28: 18-24**)*

關鍵詞：肺泡蛋白沉積症，麴菌，長期呼吸器依賴

台中榮民總醫院　內科部　胸腔內科，* 台中榮民總醫院　病理部
索取抽印本請聯絡：沈光漢醫師，台中榮民總醫院　內科部　胸腔內科，台中市中港路三段 160 號

Life-threatening Upper Airway Obstruction Caused by Massive Subcutaneous Emphysema during Mechanical Ventilation: A Case Report

Jiann-Hwa Kao, Wen-Kuang Yu, Te-Cheng Lien

Subcutaneous emphysema usually causes pain and swelling, and requires conservative treatment only. We present a case with severe subcutaneous emphysema during positive pressure mechanical ventilation. Life-threatening complications developed in our patient, including intubation difficulty due to upper airway obstruction and occult pneumothorax. We performed an infraclavicular skin incision for decompression, after which endotracheal intubation could be carried out. Computed tomography (CT) after intubation clearly revealed a collapsed extrathoracic upper airway, which was compressed by extremely inflated soft tissue. CT also showed occult pneumothorax not found in the chest X-ray. Occult pneumothorax was also managed by tube thoracostomy. We believe subcutaneous emphysema in mechanically ventilated patients should be considered an alarm sign sometimes deserving of more than conservative treatment. ***(Thorac Med 2013; 28: 25-30)***

Key words: subcutaneous emphysema, upper airway obstruction, occult pneumothorax

Introduction

Barotrauma is a common complication in ventilated patients, with an incidence of about 3% [1]. The escape of air into the extrapulmonary area can be due to pneumothorax, pneumomediastinum and subcutaneous emphysema. In contrast to pneumothorax, which was thought to be an emergency condition requiring evacuation of air immediately to prevent tension pneumothorax and mortality [2], subcutaneous emphysema used to be considered of little clinical significance and only a cosmetic problem [3].

We report a patient under mechanical ventilation support who presented with massive subcutaneous emphysema only, followed by 2 life-threatening conditions: first, upper airway obstruction secondary to a collapsed extrathoracic upper airway and second, a hidden risk of death due to occult pneumothorax, which could not be found on chest X-ray.

Case Report

An 88-year-old male with a history of hypopharyngeal squamous cell carcinoma under concurrent chemoradiation therapy presented with progressive dyspnea. Two weeks before

Department of Respiratory Therapy, Taipei Veterans General Hospital, Taipei, Taiwan
Address reprint requests to: Dr. Wen-Kuang Yu, Department of Respiratory Therapy, Taipei Veterans General Hospital, No. 201, Sec. 2, Shih-Pai Rd., Taipei 11217, Taiwan, R.O.C.

admission, magnetic resonance imaging (MRI) showed a patent trachea (Figure 1) with a suspected small residual supraglottic tumor; fibroscopy revealed palsy of the bilateral vocal cords. Because of severe stridor, emergency oral endotracheal intubation with mechanical ventilation support was first initiated, followed by tracheostomy performed smoothly with a 7.5-French tracheostomy tube. Four days after tracheostomy, the patient became agitated and tried to pull out his tracheal tube. Then, the following setting was noted on the high pressure alarm of the ventilator: FiO_2: 45%, volume assist-control mode, tidal volume: 570 ml, and PEEP: 5 cmH_2O. Respiratory distress with severe subcutaneous emphysema in the head, neck and upper trunk occurred. Dislodgement of the tracheal tube was also found and could not be corrected. We attempted to change to a 7.5-French oral endotracheal tube with laryngoscopy twice. However, the procedure was hindered by some obstacles behind the vocal cords, and desaturation progressed rapidly. Bilateral infraclavicular incisions were made emergently for severe subcutaneous emphysema. After the emergency procedure, the patient was intubated successfully with a 6.5-French endotracheal tube. We discovered severe subcutaneous emphysema on the chest X-ray only after performing intubation (Figure 2). However, much more information was found on chest computed tomography (CT), including right pneumothorax (Figure 3, arrow), a compressed extrathoracic tracheal airway (arrow heads in Figures 3 and 4A) and a patent intrathoracic airway (Figure 4B, arrow head). After thoracostomy, the patient was gradually stabilized, and was weaned from the mechanical ventilator with an 8.0-French tracheostomy tube 2 weeks later. Two months later, follow-up CT arranged at the outpatient department

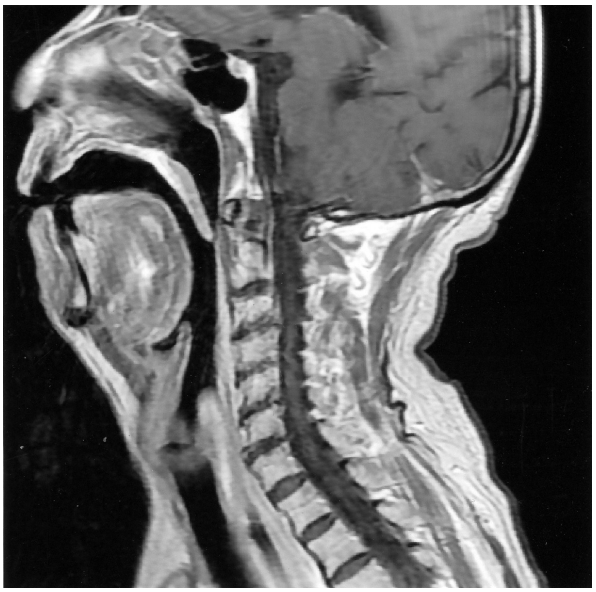

Fig. 1. Three weeks before the event, MRI of the neck revealed patency of the trachea with a diameter of 1.9 cm.

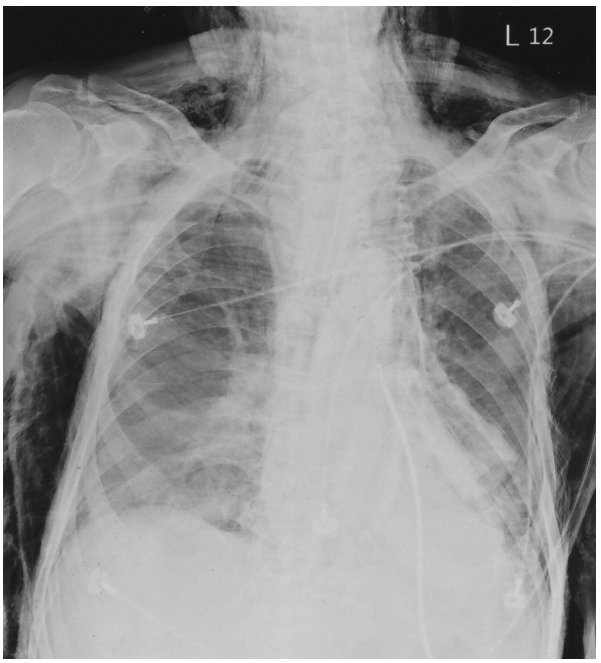

Fig. 2. Chest radiograph after intubation revealed massive subcutaneous emphysema only; signs of pneumothorax could not be found in this supine critically ill patient.

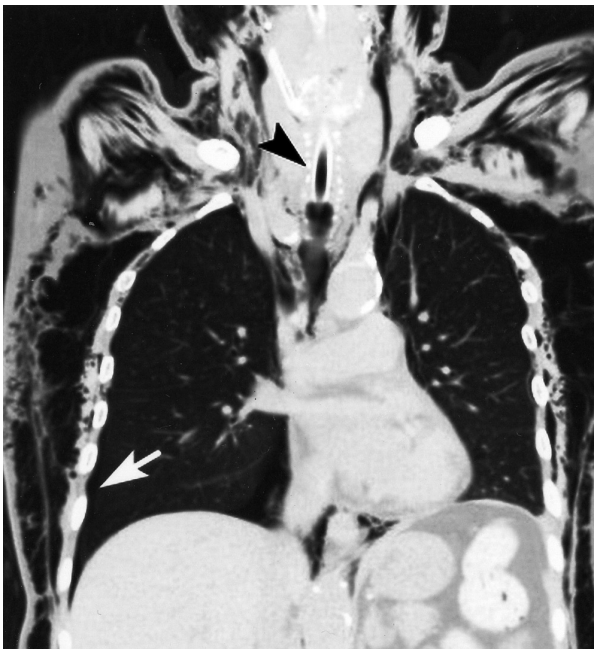

Fig. 3. Occult pneumothorax (arrow) and collapsed extrathoracic airway (arrow head) can be seen.

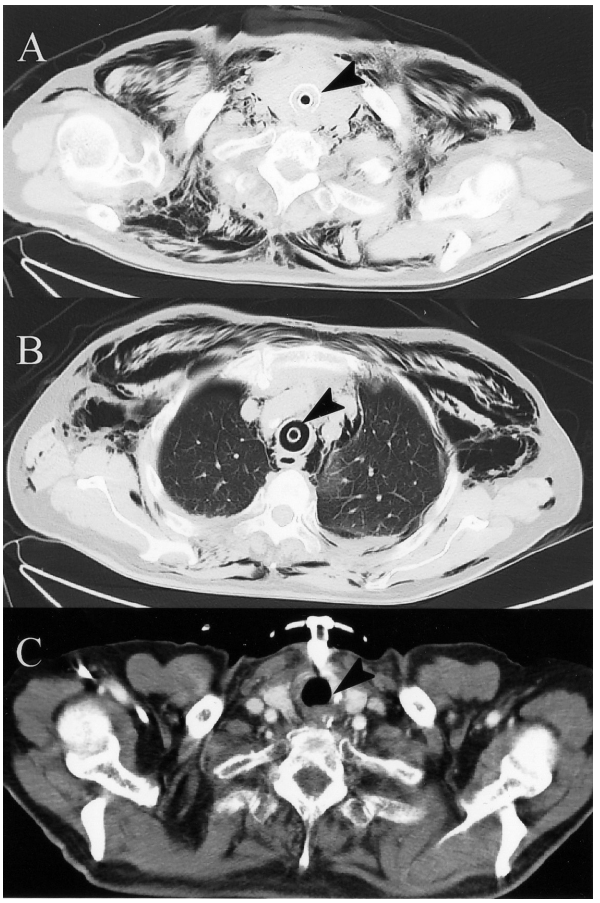

Fig. 4. (A) The extrathoracic tracheal airway (arrow head) was compressed by inflated soft tissue of the neck. (B) The difference in the diameter of the patent intrathoracic airway (arrow head, diameter of 2.0 cm) and the collapsed extrathoracic airway (arrow head in 4A, diameter of 0.9 cm) can be seen. (C) CT arranged about 2 months after the event revealed a patent upper airway (arrow, diameter of 1.8 cm) without abnormality of the adjacent organs, such as the thyroid gland.

revealed a patent upper airway (Figure 4C).

Discussion

Subcutaneous emphysema could be caused by airway trauma during intubation or by dissection of air from ruptured alveoli into the soft tissues. Possible reasons for subcutaneous emphysema include posttraumatic bronchopleural fistulae, esophageal disruptions, surgical dental extraction, childbirth, acute asthma attack and deep sea diving [3]. Although it is not unusual in patients with positive pressure mechanical ventilation, it has usually been considered a cosmetic problem and not life-threatening [3].

However, several catastrophic complications caused by massive subcutaneous emphysema have been reported, including hypoxia caused by restrictive ventilation [4-5], upper airway obstruction [6], decreased cardiac output [5] and intracranial hypertension [7] caused by decreased venous return. Although the relationship between barotrauma and pressure is still controversial [8-9], these complications occur mainly in patients with positive pressure mechanical ventilation.

Our patient presented as a typical picture of upper airway obstruction caused by subcutaneous emphysema. The CT of the chest clearly indicated the pathogenesis of this complication,

and demonstrated the difference between the diameters of the intrathoracic and extrathoracic airways, which were extrinsically compressed by extremely inflated soft tissue. We assumed that inflation of the soft tissue of the chest wall might also lead to restriction of the chest wall and lung expansion.

Management for massive subcutaneous emphysema has not been well studied, and a search of the literature found only several case reports, which revealed subcutaneous emphysema regressed after tracheostomy [5], infraclavicular "blow holes" [10-11], a large-bore subcutaneous drain [4] or microdrainage with a smaller 14-gauge penetrated catheter [12]. Our case, in which the patient survived after skin incision in the infraclavicular area, reinforced the practicality of the "blow holes" technique. All of these methods allow rapid decompression and relaxation of the stiff neck and chest wall.

Another important issue regarding the present case is the pneumothorax, which was not discovered by chest X-ray, but was only incidentally found by chest CT. For patients with mechanical ventilation, subcutaneous emphysema or pneumomediastinum were believed to reflect an increased risk of tension pneumothorax [2], which could be fatal. An imaging study to detect pneumothorax should be arranged in these high-risk patients, but because of the different distribution of air in supine patients [13], chest X-ray, with a sensitivity of only 50% [14] to 80% [15], is not a reliable examination to detect pneumothorax. In sitting patients, extrapulmonary air accumulates in the apex of the lung and causes a superior-lateral visceral pleural stripe. For supine patients, in contrast, air would be in the non-dependent sites, including the anteromedial and subpulmonic recesses [13], which could be missed on chest X-ray.

For early diagnosis of occult pneumothorax, chest CT is the "gold standard" examination, but practicality is limited by exposure to radiation and the high risk during transportation. The role of chest sonography is under evaluation, but ultrasound can be blocked by extrapulmonary air and has its limitations. Based on the above, we arranged chest CT and found this hidden life-threatening situation.

Studies on the management of occult pneumothorax have yielded controversial results. Enderson *et al* [16] revealed higher rates of tension pneumothorax in patients not treated with thoracostomy. Forty mechanically ventilated patients with occult pneumothorax were enrolled and randomized to tube thoracostomy (n=19) and observation (n=21). In patients treated with observation, progression of pneumothorax was found in 38.1% and tension pneumothorax in 14.3%. In contrast, no patients receiving thoracostomy suffered from major complications. The OPTICC study [17] included 24 patients with positive pressure ventilation and occult pneumothorax. Thirteen patients were randomized to the observation group, and the other patients received tube thoracostomy; 30.1% of those thirteen patients had a chest tube inserted non-urgently, and mortality was similar between the groups (22% of 11 patients with tube drainage and 15% of 13 patients with observation). Even with the limited published findings on treatment, we still treated our patient with thoracostomy. After treatment, the patient gradually stabilized and was transferred to an ordinary ward once free from other events.

Conclusion

The development of massive subcutaneous emphysema in a ventilated patient is an alarm-

ing problem which should not be neglected. Complications including restriction of the chest wall and compression of the upper airway could occur because of extrinsic compression by extremely inflated soft tissues. In these situations, emergency decompression via a large bore drainage tube or infraclavicular "blow hole" should be performed, although only a few case reports on management have been published. Moreover, occult pneumothorax in patients at a high risk should be kept in mind. Ultrasonography or CT should be arranged because of the inadequate sensitivity of chest X-ray in supine critically ill patients. Tube thoracostomy in these patients is still controversial, so before further evidence is found, we should arrange drainage of air in order to prevent life-threatening tension pneumothorax.

References

1. Esteban A, Anzueto A, Frutos F, *et al*. Characteristics and outcomes in adult patients receiving mechanical ventilation: a 28-day international study. JAMA 2002; 287(3): 345-55.
2. Zimmerman JE, Dunbar BS, Klingenmaier CH. Management of subcutaneous emphysema, pneumomediastinum, and pneumothorax during respirator therapy. Crit Care Med 1975; 3(2): 69-73.
3. Maunder RJ, Pierson DJ, Hudson LD. Subcutaneous and mediastinal emphysema. Pathophysiology, diagnosis, and management. Arch Intern Med 1984; 144(7): 1447-53.
4. Kelly MC, McGuigan JA, Allen RW. Relief of tension subcutaneous emphysema using a large bore subcutaneous drain. Anaesthesia 1995; 50(12): 1077-9.
5. Conetta R, Barman AA, Iakovou C, *et al*. Acute ventilatory failure from massive subcutaneous emphysema. Chest 1993; 104(3): 978-80.
6. Sanford TJ Jr, Shapiro HM, Gallick MN. Pericardial and subcutaneous air after maxillary surgery. Anesth Analg 1987; 66(3): 277-9.
7. Coelho JC, Tonnesen AS, Allen SJ, *et al*. Intracranial hypertension secondary to tension subcutaneous emphysema. Crit Care Med 1985; 13(6): 512-3.
8. Boussarsar M, Thierry G, Jaber S, *et al*. Relationship between ventilatory settings and barotrauma in the acute respiratory distress syndrome. Intensive Care Med 2002; 28(4): 406-13.
9. Weg JG, Anzueto A, Balk RA, *et al*. The relation of pneumothorax and other air leaks to mortality in the acute respiratory distress syndrome. NEJM 1998; 338(6): 341-6.
10. Herlan DB, Landreneau RJ, Ferson PF. Massive spontaneous subcutaneous emphysema. Acute management with infraclavicular "blow holes". Chest 1992; 102(2): 503-5.
11. Cesario A, Margaritora S, Porziella V, *et al*. Microdrainage via open technique in severe subcutaneous emphysema. Chest 2003; 123: 2161-2.
12. Beck PL, Heitman SJ, Mody CH. Simple construction of a subcutaneous cathether for the treatment of severe subcutaneous emphysema. Chest 2002; 121: 647-9.
13. Tocino IM, Miller MH, Fairfax WR. Distribution of pneumothorax in the supine and semirecumbent critically ill adult. AJR 1985; 144(5): 901-5.
14. Omar HR, Abdelmalak H, Mangar D, *et al*. Occult pneumothorax, revisited. J Trauma Manag Outcomes 2010; 4: 12-7.
15. Wall SD, Federle MP, Jeffrey RB, *et al*. CT diagnosis of unsuspected pneumothorax after blunt abdominal trauma. AJR 1983; 141(5): 919-21.
16. Enderson BL, Abdalla R, Frame SB, *et al*. Tube thoracostomy for occult pneumothorax: a prospective randomized study of its use. J Trauma 1993; 35(5): 726-9.
17. Ouellet JF, Trottier V, Kmet L, *et al*. The OPTICC trial: a multi-institutional study of occult pneumothoraces in critical care. Am J Surg 2009; 197(5): 581-6.

於呼吸器使用時，嚴重的皮下氣腫造成之致命的上呼吸道阻塞：個案報告

高建華　余文光　連德正

皮下氣腫一向被認為只會影響到美觀，而且只需要保守性的治療。我們提出一個病患在正壓呼吸器使用的期間，產生了嚴重的皮下氣腫。很重要地，致命的併發症發生在我們的病患身上，包括了上呼吸道阻塞造成的插管困難，和隱藏性的氣胸。急救過後的胸部電腦斷層上顯示出，因為皮下軟組織嚴重的充氣，而被壓扁的胸廓外上呼吸道。我們緊急地在病人的鎖骨下方，進行皮膚切開以便減壓，之後，病人順利插入氣管內管，電腦斷層上亦顯示出 X 光上無法發現的隱藏性氣胸，氣胸也趕緊小心處理。我們相信，在使用呼吸器的病人中，皮下氣腫是一個警訊，而且需要的絕對不只是保守性治療。*(胸腔醫學* ***2013; 28: 25-30)***

關鍵詞：皮下氣腫，上呼吸道阻塞，隱藏性氣胸

台北榮民總醫院　呼吸治療科
索取抽印本請聯絡：余文光醫師，台北榮民總醫院　呼吸治療科，台北市北投區石牌路二段 201 號

Tracheobronchomegaly and Ankylosing Spondylitis: A Case Report and Literature Review

Meng-Zhi Han, Han-Yu Chang

Tracheobronchomegaly, also called Mounier-Kuhn syndrome, is a distinct condition that involves marked dilation of the trachea and central bronchi, in association with chronic respiratory tract infections. It probably results from a congenital defect of the elastic and muscle fibers within the tracheal and bronchial walls. Secondary tracheobronchomegaly associated with Marfan syndrome, connective tissue diseases, ataxia-telangiectasia, ankylosing spondylitis, cutis laxa, light chain deposition disease, and others, has also been described. In patients with ankylosing spondylitis, the most commonly described pulmonary manifestations are upper lobe fibrosis, mycetoma formation, and pleural thickening. Tracheobronchomegaly is a rare finding in ankylosing spondylitis. We reported a male patient with both tracheobronchomegaly and ankylosing spondylitis. ***(Thorac Med 2013; 28: 31-37)***

Key words: tracheobronchomegaly, Mounier-Kuhn syndrome

Introduction

Tracheobronchomegaly, also called Mounier-Kuhn syndrome, is a distinct condition that involves marked dilation of the trachea and central bronchi, in association with chronic respiratory tract infections [1]. Because of the weakened trachea, mucosal herniations may also develop between the tracheal rings in some patients, leading to tracheal diverticulosis and retention of secretions. The airways distal to the fourth-order and fifth-order division are usually normal in diameter [2]. Tracheobronchomegaly is more common in men and is typically diagnosed in the 3rd or 4th decades of life [3]. The etiology is uncertain, but it probably results from a congenital defect of the elastic and muscle fibers within the tracheal and bronchial walls. Previous authors have suggested a congenital nature of the disease, since it is sometimes associated with Ehlers-Danlos syndrome in adults and cutis laxa in children [4]. The reported incidence of pleuropulmonary involvement in ankylosing spondylitis varies from 0% to 30% [5]. Pleuropulmonary manifestations include upper lobe fibrosis, mycetoma formation, pleural thickening, pleural effusion and empyema, pneumothorax and cor pulmonale. Tracheobronchomegaly associated with ankylosing spondilitis was first described

Division of Pulmonary Medicine, Department of Internal Medicine, National Cheng Kung University Hospital, Tainan, Taiwan
Address reprint requests to: Dr. Han-Yu Chang, Division of Pulmonary Medicine, Department of Internal Medicine, National Cheng Kung University Hospital, No 138, Sheng-Li Rd. Tainan 704, Taiwan

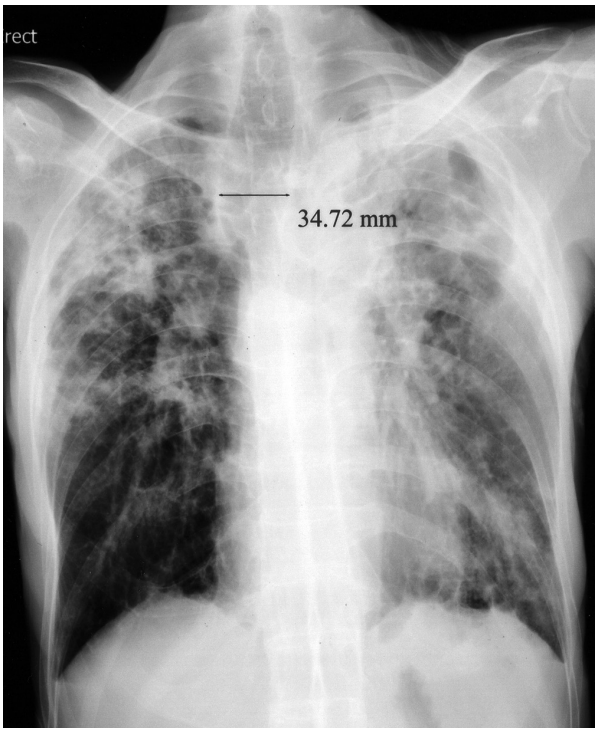

(A)

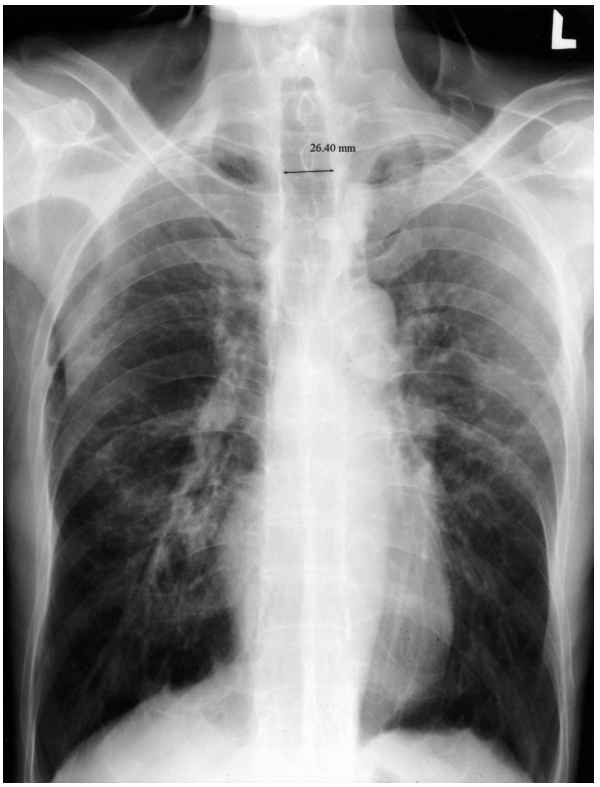

(B)

Fig. 1. Chest radiograph showed tracheomegaly with a diameter of 34.72 mm in 2011 (A) and tracheomegaly with a diameter of 26.4 mm in 2007 (B)

by Padley *et al* in 1991 [6]. The clinical presentation of the syndrome varies widely. The grossly enlarged but weakened airways and inefficient cough mechanisms affect mucociliary clearance, which leads to mucus retention with resultant recurrent pneumonia, bronchiectasis, and fibrosis. On a plain chest radiograph, the increased caliber of the central airways may be visible, but the diagnosis is usually made with a computed tomography (CT) scan. Treatment of Mounier-Kuhn syndrome is limited to physiotherapy to assist in clearing secretions, and appropriate antibiotics during infectious exacerbations. Severe cases that involved the use of stenting of the airways have been reported [7].

Case Report

A 59-year-old male, a businessman, had ankylosing spondylitis and bronchiectasis. He had experienced an increased expectoration of sputum that became purulent during infectious exacerbations, sometimes with bloody sputum, for more than 4 years. He complained of an increase in his productive cough beginning the year before. He had intermittent fever and blood-tinged sputum for 1 month and visited our chest outpatient department. He denied fever, wheezing, chest pain, and weight loss. Chest radiography was performed and showed tracheomegaly with transverse diameters of the trachea of 34.72 mm, and bilateral upper lobe and left

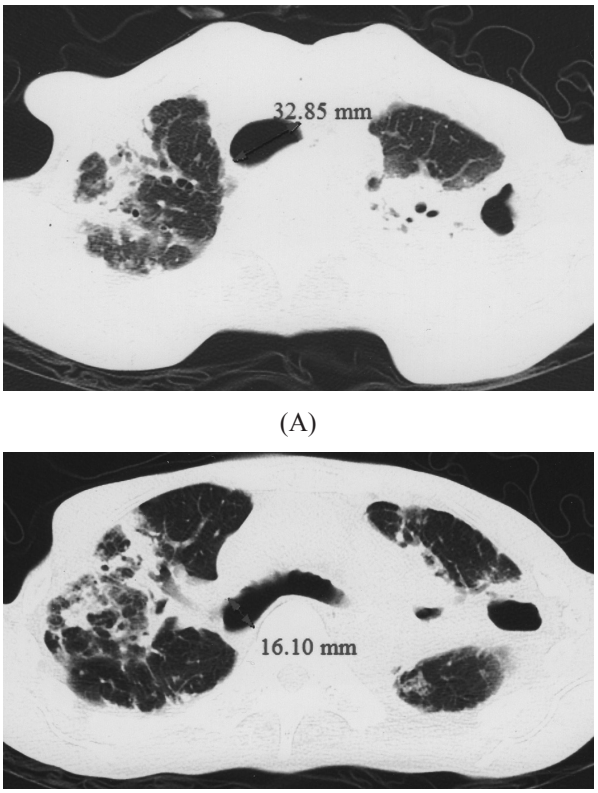

(A)

(B)

Fig. 2. CT scan of the chest showed a massively dilated trachea with a diameter of 32.85 mm (A) and dilated main stem bronchi (B)

lower lobe pneumonia (Figure 1A). His chest radiography 4 years ago also showed dilated trachea with transverse diameters of the trachea of 26.4 mm (Figure 1B).

A CT scan of the chest was performed, and showed bilateral upper lobe consolidation with cavitation of the left upper lobe and a massively dilated trachea (Figure 2A) and main stem bronchi (Figure 2B). The pulmonary function test showed a moderate restrictive ventilatory defect, with FVC and FEV_1 at 44% and 53% of predictive value, respectively. Bronchoscopy was performed, and showed tracheomegaly with excessive dynamic change at the inspiratory and expiratory phases (Figure 3A), and an obvious bronchial orifice, even at the sub-segmental orifice (Figure 3B).

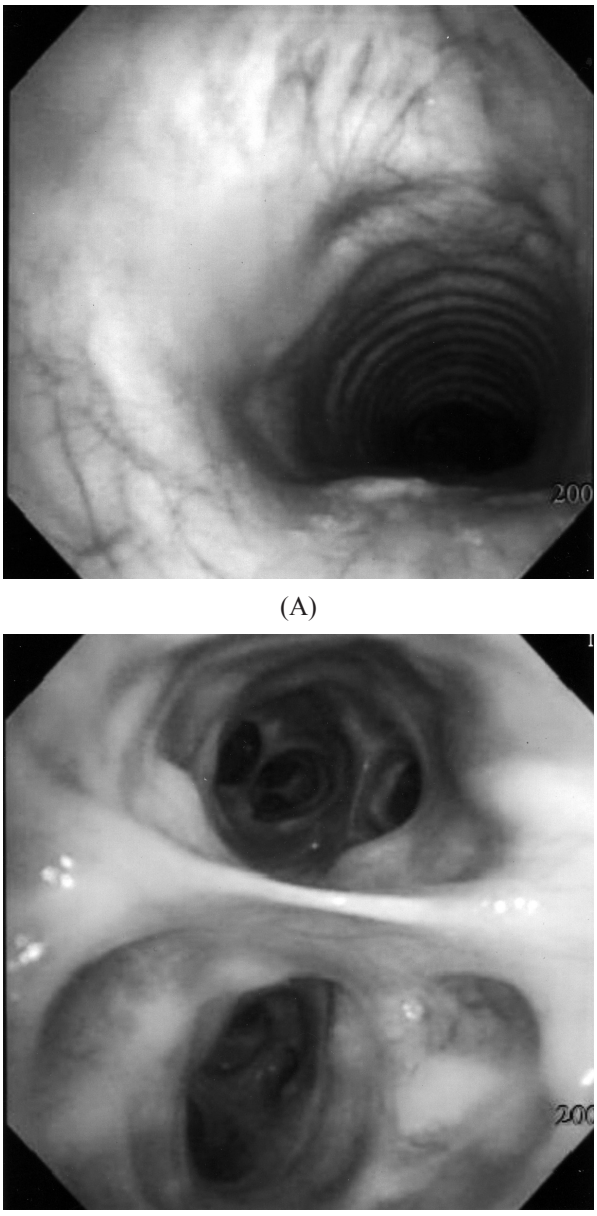

(A)

(B)

Fig. 3. Bronchoscope showed tracheomegaly (A), and an obvious bronchial orifice at the sub-segmental orifice (B)

Discussion

Congenital tracheobronchomegaly, also called Mounier-Kuhn syndrome, is a rare clini-

cal and radiological entity described for the first time by Mounier and Kuhn in 1932 [8]. This syndrome is characterized by marked widening of the trachea and major bronchi, which may be associated with tracheal diverticulosis, bronchiectasis, and lower respiratory tract infection. The clinical presentation of the syndrome varies widely. Severity ranges from a chronic cough to severe respiratory failure with a need of mechanical ventilation. The most frequent signs are chronic cough and sputum production with recurrent respiratory tract infections.

The etiology of Mounier-Kuhn syndrome is uncertain, but it is believed to be due to a congenital defect or atrophy of the elastic and smooth muscle tissue of the trachea and main bronchi [9]. Sacculations and the formation of diverticula between the cartilaginous rings develop, commonly in the posterior part, due to the loss of inherent tracheal wall support [10-11]. The airways distal to the fourth-order and fifth-order division are usually normal in diameter. The syndrome is male-predominant, and patients usually present in their 3rd and 4th decades of life, although some cases have been reported at ages ranging from 18 months to 76 years [1,12]. Disorders that cause severe fibrosis of the upper lobes, such as sarcoidosis, usual interstitial pneumonia and cystic fibrosis, may lead to tracheal traction and result in tracheal enlargement [11]. A familial group has been described and a possible autosomal-dominant mode of inheritance suggested [13]. Secondary tracheobronchomegaly has also been described in association with Marfan syndrome, Ehlers-Danlos syndrome, Kenny-Caffey syndrome, ataxia-telangiectasia, Brachmann-de Lange syndrome, Bruton-type agammaglobulinemia, ankylosing spondylitis, rheumatoid arthritis, cutis laxa, and light chain deposition disease [2,14-17]. Most cases, however, are sporadic and show no evidence of associated connective tissue disease.

The incidence of pleuropulmonary involvement in ankylosing spondylitis varies from 0% to 30%. The most common thoracic finding is ankylosis of the costovertebral joints limiting chest expansion. Pleuropulmonary manifestations are reported less commonly and include upper lobe fibrosis, mycetoma formation, pleural thickening, pleural effusion and empyema, pneumothorax, and cor pulmonale. Tracheobronchomegaly in association with ankylosing spondylitis was first described by Padley *et al* in 1991 [6]. In a study of plain radiographs and thoracic CT of patients with ankylosing spondylitis, 2 of 18 patients had saber sheath trachea and increased coronal and sagittal tracheal diameters [5]. Tracheobronchomegaly and ankylosing spondylitis may represent part of a spectrum of connective tissue disorders, and their association may not be by chance, but further investigations are required for confirmation [6].

Pulmonary function tests of patients with tracheobronchomegaly may reveal an obstructive pattern, as well as increased residual volume and hyperinflation with a decreased diffusion capacity of carbon monoxide if lung parenchymal diseases are present. In advanced cases, a restrictive pattern secondary to fibrosis will be predominant. Despite the severity of the disorder, pulmonary function tests can be within normal range in some cases [18].

Breatnach *et al* established the normal range of the internal coronal and sagittal diameters of the trachea in adult patients without clinical or radiographic evidence of respiratory disease. They found the upper limits were 25 and 27 mm (coronal and sagittal, respectively) in men and 21 and 23 mm in women. The lower limit for both dimensions was 13 mm in men

and 10 mm in women. Tracheal dimensions greater than or less than these values indicate pathologic tracheal widening or narrowing [19].

The increased caliber of the central airways may be visible on plain chest x-ray, especially in the lateral view. For an adult, a diameter of the trachea, right main bronchus, and left main bronchus that exceeds 30 mm, 24 mm, and 23 mm, respectively, on a standard chest x-ray or bronchogram is diagnostic of tracheobronchomegaly. On CT scan, the diagnosis of Mounier-Kuhn syndrome in women is made when the transverse and sagittal diameters of the trachea exceed 21 mm and 23 mm, respectively, and when the transverse diameters of the right and left main bronchi exceed 19.8 mm and 17.4 mm, respectively. In men, Mounier-Kuhn syndrome is diagnosed when the transverse and sagittal diameters of the trachea exceed 25 mm and 27 mm, respectively, and when the transverse diameters of the right and left main bronchi exceed 21.1 mm and 18.4 mm, respectively [20]. Chest CT scan allows for evaluation of the full extent of the disease, and the presence of associated tracheal diverticulosis or areas of bronchiectasis.

Tracheobronchomegaly has been classified into 3 subtypes. In type 1, there is a relatively subtle symmetrically diffuse enlargement of the trachea and major bronchi. Type 2 has more obvious enlargement with a bizarre eccentric configuration, and diverticula may also be present. In type 3, diverticula or sacculations extend to the distal bronchi [1].

Treatment of Mounier-Kuhn syndrome is limited to physiotherapy to assist in clearing secretions and appropriate antibiotics during infectious exacerbations. Cessation of smoking is highly beneficial, as is minimizing exposure to industrial and occupational irritants and pollutants. There is little role for surgery because of the diffuse nature of the disease. There are a few case reports in which a Y-shaped tracheobronchial stent placement helped the trachea remain open, with significant clinical improvement [21-22]. A few cases of lung transplantation in Mounier-Kuhn syndrome have been reported, but there is no proven benefit with regard to morbidity and mortality [23]. Inhaled bronchodilators and corticosteroids are ineffective for the treatment of this syndrome [24].

References

1. Schwartz M, Rossoff L. Tracheobronchomegaly. Chest 1994; 106(5): 1589-90.
2. Blake MA, Clarke PD, Fenlon HM. Thoracic case of the day. Mounier-Kuhn syndrome (tracheobronchomegaly). AJR Am J Roentgenol 1999; 173(3): 822, 824-5.
3. Dunne MG, Reiner B. CT features of tracheobronchomegaly. J Comput Assist Tomogr 1988; 12(3): 388-91.
4. Aaby GV, Blake HA. Tracheobronchiomegaly. Ann Thorac Surg 1966; 2(1): 64-70.
5. Fenlon HM, Casserly I, Sant SM, *et al*. Plain radiographs and thoracic high-resolution CT in patients with ankylosing spondylitis. AJR Am J Roentgenol 1997; 168(4): 1067-72.
6. Padley S, Varma N, Flower CD. Tracheobronchomegaly in association with ankylosing spondylitis. Clin Radiol 1991; 43(2): 139-41.
7. Lafaye-Robin ML, Muir JF, Kouziaeff N, *et al*. Treatment of tracheobronchomegaly using the Freitag prosthesis. Rev Mal Respir 1998; 15(3): 291-4.
8. Smith DL, Withers N, Holloway B, *et al*. Tracheobronchomegaly: an unusual presentation of a rare condition. Thorax 1994; 49(8): 840-1.
9. Katz I, Levine M, Herman P. Tracheobronchiomegaly. The Mounier-Kuhn syndrome. Am J Roentgenol Radium Ther Nucl Med 1962; 88: 1084-94.
10. Himalstein MR, Gallagher JC. Tracheobronchiomegaly. Ann Otol Rhinol Laryngol 1973; 82(2): 223-7.
11. Marom EM, Goodman PC, McAdams HP. Diffuse abnormalities of the trachea and main bronchi. AJR Am J Roent-

genol 2001; 176(3): 713-7.
12. Hunter TB, Kuhns LR, Roloff MA, *et al*. Tracheobronchiomegaly in an 18-month-old child. Am J Roentgenol Radium Ther Nucl Med 1975; 123(4): 687-90.
13. Johnston RF, Green RA. Tracheobronchiomegaly. Report of five cases and demonstration of familial occurrence. Am Rev Respir Dis 1965; 91: 35-50.
14. Lazzarini-de-Oliveira LC, Costa de Barros Franco CA, Gomes de Salles CL, *et al*. A 38-year-old man with tracheomegaly, tracheal diverticulosis, and bronchiectasis. Chest 2001; 120(3): 1018-20.
15. Celenk C, Celenk P, Selcuk MB, *et al*. Tracheomegaly in association with rheumatoid arthritis. Eur Radiol 2000; 10(11): 1792-4.
16. Van Schoor J, Joos G, Pauwels R. Tracheobronchomegaly--the Mounier-Kuhn syndrome: report of two cases and review of the literature. Eur Respir J 1991; 4(10): 1303-6.
17. Sane AC, Effmann EL, Brown SD. Tracheobronchiomegaly. The Mounier-Kuhn syndrome in a patient with the Kenny-Caffey syndrome. Chest 1992; 102(2): 618-9.
18. Ghanei M, Peyman M, Aslani J, *et al*. Mounier-Kuhn syndrome: a rare cause of severe bronchial dilatation with normal pulmonary function test: a case report. Respir Med 2007; 101(8): 1836-9.
19. Breatnach E, Abbott GC, Fraser RG. Dimensions of the normal human trachea. AJR Am J Roentgenol 1984; 142(5): 903-6.
20. Menon B, Aggarwal B, Iqbal A. Mounier-Kuhn syndrome: report of 8 cases of tracheobronchomegaly with associated complications. South Med J 2008; 101(1): 83-7.
21. Collard P, Freitag L, Reynaert MS, *et al*. Respiratory failure due to tracheobronchomalacia. Thorax 1996; 51(2): 224-6.
22. Giannoni S, Benassai C, Allori O, *et al*. Tracheomalacia associated with Mounier-Kuhn syndrome in the intensive care unit: treatment with Freitag stent. A case report. Minerva Anestesiol 2004; 70(9): 651-9.
23. Shah SS, Karnak D, Mason D, *et al*. Pulmonary transplantation in Mounier-Kuhn syndrome: a case report. J Thorac Cardiovasc Surg 2006; 131(3): 757-8.
24. Falconer M, Collins DR, Feeney J, *et al*. Mounier-Kuhn syndrome in an older patient. Age Ageing 2008; 37(1): 115-6.

氣管支氣管巨大症與僵直性脊椎炎：病例報告及文獻回顧

韓孟志　張漢煜

氣管支氣管巨大症又被稱為 Mounier-Kuhn 症候群，是一種在氣管及支氣管會有顯著擴張且合併有慢性呼吸道感染的獨特疾病。其病因源於氣管及支氣管壁的彈性及肌肉組織之先天性缺陷。氣管支氣管巨大症亦可和馬凡氏症候群，結締組織疾病，毛細血管擴張性運動失調，僵直性脊椎炎，皮膚鬆弛症及輕鏈沉積病等疾病有所關聯。在此，我們報告一個有氣管支氣管巨大症合併僵直性脊椎炎的男性案例。*(胸腔醫學* ***2013; 28: 31-37)***

關鍵詞：氣管支氣管巨大症，Mounier-Kuhn 症候群

成功大學附設醫院內科部　胸腔內科
索取抽印本請聯絡：張漢煜醫師，成功大學附設醫院內科部　胸腔內科，704 台南市北區勝利路 138 號

Pitfall in Diagnosing Lymphoepithelioma-like Carcinoma of the Lung: A Case Report and Literature Review

Yi-Mou Wu, Gwan-Han Shen, Jeng-Yuan Hsu

Lymphoepithelioma-like carcinoma (LELC) of the lung is a rare form of lung cancer. The diagnosis requires tissue biopsy for histological and immunohistochemical stain. The prognosis is better than for other non-small cell lung cancers (NSCLC). We report a 60 year-old man who presented with a central pulmonary mass and pleural effusion. Scanty tissue from endobronchial ultrasonography with transbronchial needle aspiration (EBUS-TBNA) resembled squamous cell carcinoma morphologically. But biopsy via thoracoscopy showed high grade tumor cells arranged in a solid sheet pattern, infiltrated by varying numbers of lymphocytes. *In situ* hybridization for Epstein-Barr virus (EBV) encoded RNA showed localization of EBV genomes within the nuclei of tumor cells. LELC of the lung was diagnosed, and the patient received platinum-based chemotherapy. ***(Thorac Med 2013; 28: 38-43)***

Key words: lymphoepithelioma-like carcinoma (LELC), endobronchial ultrasonography transbronchial needle aspiration, squamous cell carcinoma, diagnosis

Introduction

Lymphoepithelioma originally is a poorly differentiated nasopharyngeal carcinoma (NPC) characterized by prominent infiltration of lymphocytes in the area involved by the tumor. Primary carcinoma with the same histological finding has been reported in foregut derivatives, including the oral cavity, salivary glands, thymus, lungs, and stomach, and has been termed lymphoepithelioma-like carcinoma (LELC). Begin *et al* first reported a primary LELC of the lung in 1987 and demonstrated the relationship between LELC of the lung and Epstein-Barr virus (EBV) infection [1]. The patients are predominantly East Asians and the prognosis is better than for other NSCLC [2].

Case Report

A 60 year-old man, an ex-smoker with a 40 pack-year smoking history, presented with progressive dyspnea and hemoptysis for 1 week. Chest X-ray film showed right-side pleural effusion and an enlarged azygos node (Figure 1). Chest computed tomography revealed a central

Division of Chest Medicine, Department of Internal Medicine, Taichung Veterans General Hospital, Taichung, Taiwan
Address reprint requests to: Dr. Gwan-Han Shen, Division of Chest Medicine, Department of Internal Medicine, Taichung Veterans General Hospital, No. 160, Section 3, Chung-Kang Road, Taichung, Taiwan

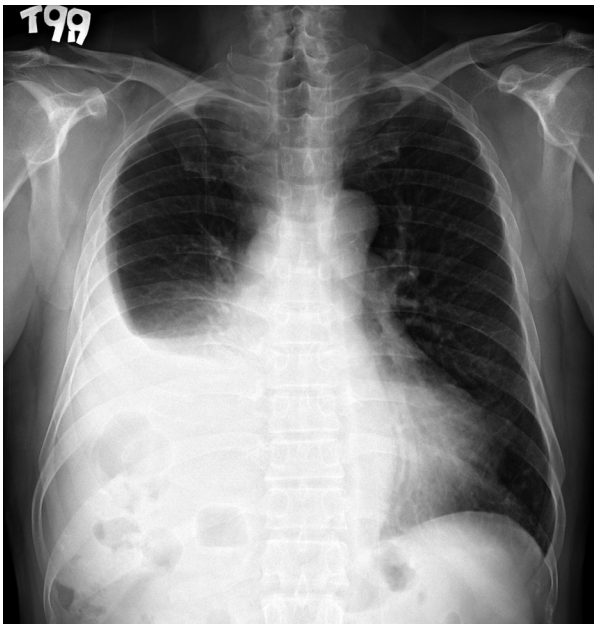

Fig. 1. Right-side pleural effusion and an enlarged azygos node.

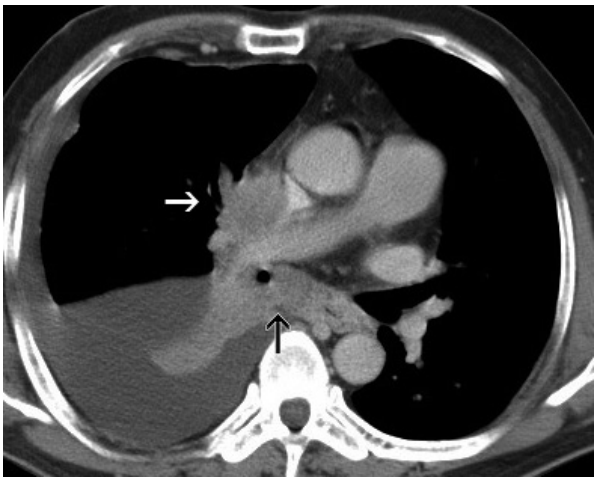

Fig. 2. Central pulmonary mass with mediastinal invasion (white arrow), multiple mediastinal lymph nodes, right lower lobe collapse and pleural effusion.

pulmonary mass with mediastinal invasion, multiple mediastinal lymph nodes, right lower lobe collapse, and right-side pleural effusion (Figure 2).

Hematological findings were as follows:

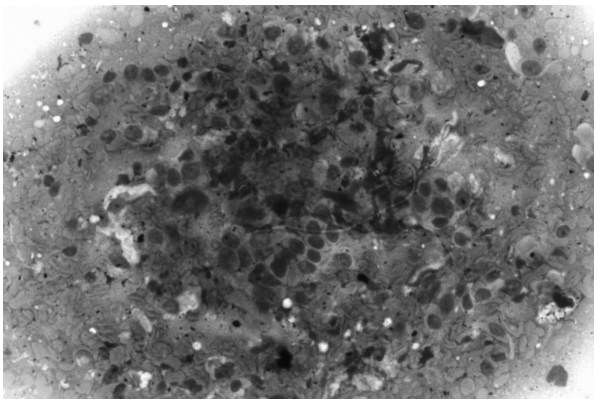

Fig. 3. Large cells with a high nucleus to cytoplasm ratio, prominent nuclei and glassy cytoplasm-like squamous cells morphologically. (Liu's stain, ×200)

hemoglobin 12.1 g/dL, platelet count 177000/ul and white blood cell count 6500/ul with a differential of 84.8% neutrophils, 8.4% lymphocytes, and 6.2% monocytes. Plasma biochemistry values were as follows: sodium 136 mEq/l, potassium 3.7 mEq/l, blood urine nitrogen 12 mg/dl, creatinine 1 mg/dl, aspartate aminotransferase 40 U/l, alanine aminotrasferase 32 U/l, lactate dehydrogenase 182 U/l, and total protein 7.9 g/dl. Pleural effusion analysis and biochemistry values were as follows: red blood cells 1900/ul, white blood cells 1910/ul with a differential of 79% lymphocytes, 1% neutrophils and 20% other cells, lactate dehydrogenase 125U/l, protein 4800 mg/dl, and glucose 112 mg/dl. There were negative results for malignant cells.

Traditional bronchoscopy revealed narrowing of the right intermediate bronchus and biopsy showed only fibrotic tissue. Endobronchial ultrasonography (EBUS) disclosed several mediastinal lymphadenopathies in the right pretracheal region and subcarina area. A few cells with a squamous cell carcinoma (SCC)-like morphology (Figure 3) were obtained via transbronchial needle aspiration (TBNA), but they

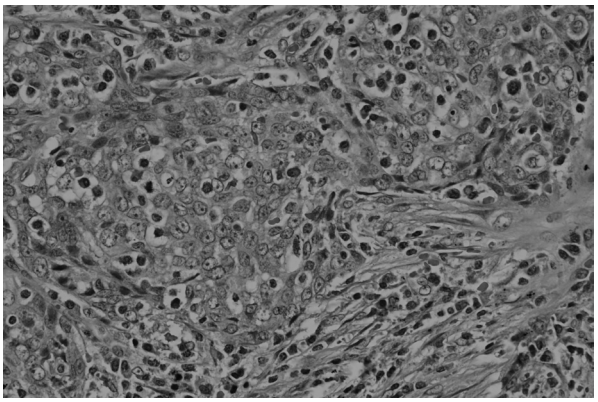

Fig. 4. High-grade tumor cells arranged in a solid sheet pattern, infiltrated by varying numbers of lymphocytes (Hematoxylin and eosin stain, ×200)

were not diagnostic.

Video-assisted thoracoscopy was arranged for further biopsy and the results showed diffuse thickening with hyperemic change in the right-side pleura. Dense adhesion in the right lower paratracheal and subcarinal area was found. Biopsies taken from these areas revealed tissue composed of high-grade tumor cells arranged in a solid sheet pattern, infiltrated by varying numbers of lymphocytes (Figure 4). *In situ* hybridization for EBV-encoded RNA (EBER) showed localization of EBV genomes within the nuclei of tumor cells. In the immunohistochemical exam, the tumor cells showed diffuse and strong staining for p63, but were negative for CK7 and TTF-1. (Figure 5). The histopathological and immunohistochemical stain features of this specimen resembled LELC. The nasopharyngeal survey was negative. LELC of the lung, T4N2M0, stage IIIB was confirmed. The patient received monthly systemic chemotherapy with cisplatin and etoposide. He achieved stable disease after 2 courses of systemic chemotherapy (Figure 6).

Discussion

LELC of the lung is identical histologically to undifferentiated NPC, and has histological features of undifferentiated carcinoma associated with prominent lymphoid stroma, and ultrastructural features of SCC [1]. LELC of the lung is a subtype of large cell carcinoma of the lung, according to the new World Health Organization histologic classification of lung tumors [3]. LELC of the lung frequently manifests as a centrally located tumor with lymph node involvement and vascular and bronchial encasement [4].

Both fine needle aspiration cytology of the tumor cells and immunohistochemical staining patterns have been used to diagnose LELC [5]. EBUS has provided a final diagnosis in 78% of patients with tumor in the mediastinum and in more than half of patients with enlarged lymph nodes, despite previous work-ups [6]. However, relatively scanty tissue from fine needle aspiration may limit the accuracy of this technique. Immunohistochemical staining using a combination of thyroid transcription factor 1 (TTF-1), napsin A, p63, and cytokeratin 5/6 allows subclassification of poorly differentiated NSCLCs in small lung biopsies in most cases [7]. In SCC, TTF-1 was negative and p63 was positive in 15 biopsies [7]. The largest reported cohort of patients with LELC of the lung, involving 52 Asian patients, showed the same immunohistochemical staining characteristics (negative for TTF-1 and positive for p63), and all had positive results from *in situ* hybridization for EBERs, confirming the association of EBV infection with pulmonary LELC in Asians [8]. In LELC of the lung, scanty tissue from fine needle aspiration may resemble SCC. Differentiation required larger tissue samples for

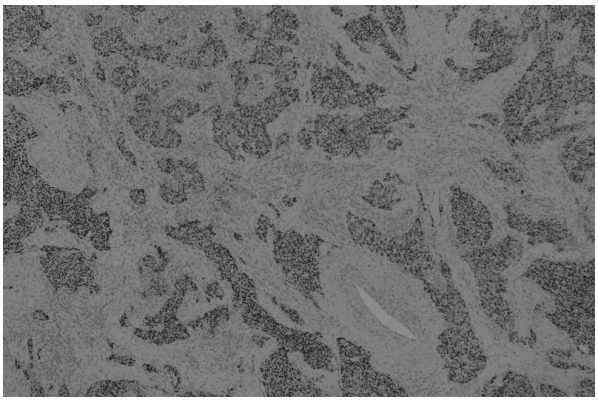

(A)

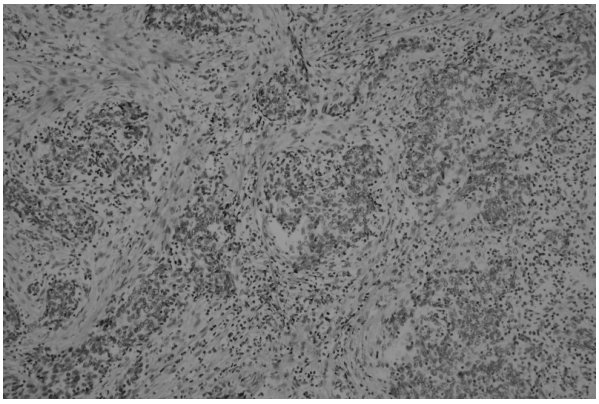

(B)

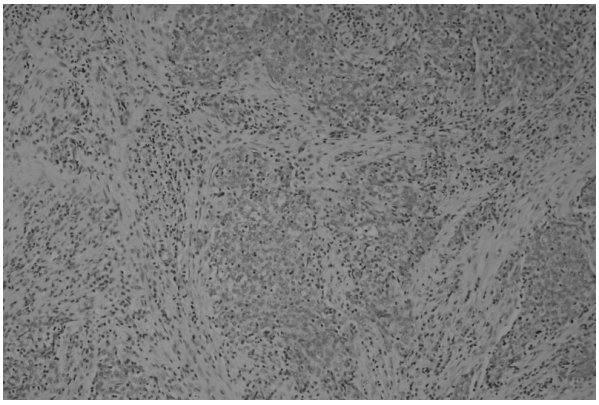

(C)

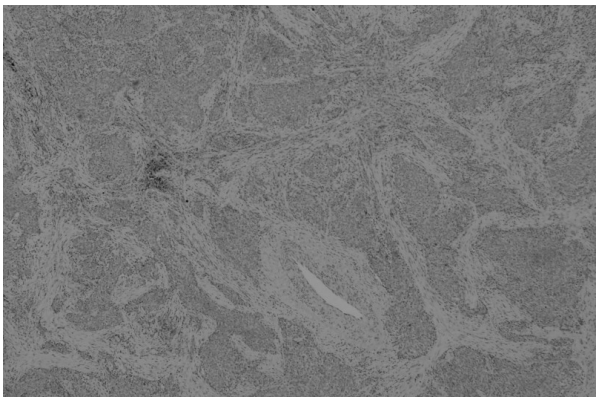

(D)

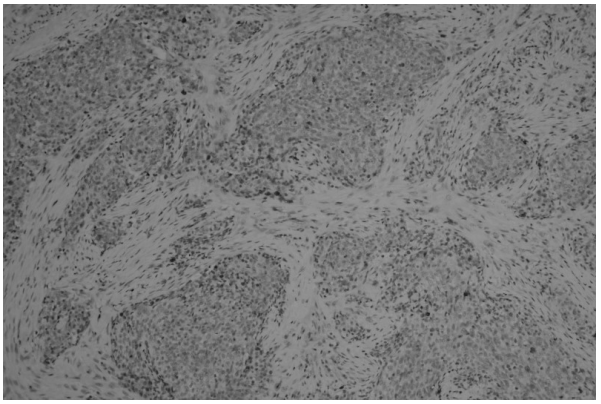

(E)

Fig. 5. A: p63 (positive), B: EBER (weak positive), C: CK7 (negative), D: TTF-1 (negative), E: CD-5 (partial positive in lymphocytes)

histological and *in situ* hybridization for EBERs [9]. Endoscopic examination of the nasopharynx should be performed to rule out metastatic LELC from the nasopharynx.

For early-stage LELC of the lung, surgical resection is the primary management to obtain a cure. For advanced LELC of the lung, multimodality treatments, including chemotherapy, surgery and radiation therapy, have been used. Platinum-based doublets commonly used for NSCLC have a good disease control rate, ranging from 77.8% to 100% [8]. Combination chemotherapy, as for NPC, with cisplatin and 5-fluorouracil has shown a 71.4% partial response rate [10]. Another study reported patients with LELC had significantly better 5-year survival than those with non-LELC, NSCLC stage III/IV disease (60.6% vs. 21.4%, $p < 0.05$) [11].

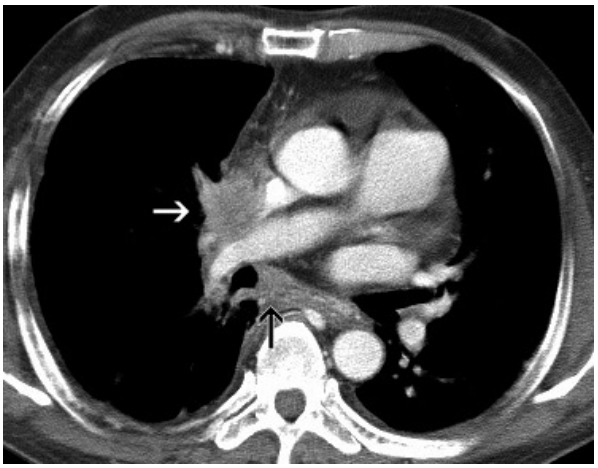

Fig. 6. Tumor volume did not decrease more than 50% (white arrow), but the size of the lymph nodes decreased (black arrow), the pleural effusion resolved, and the right lower lobe re-expanded after 2 courses of systemic chemotherapy.

The tiny lymph node tissue sample obtained from our patient via EBUS-TBNA showed scanty cells with a squamous cell morphology. LELC may be diagnosed as poorly differentiated carcinoma or SCC by cytology alone. LELC of the lung should be considered in the differential diagnosis of Asians who have a centrally located tumor with a large poorly differentiated carcinoma morphology. Further immunohistochemical staining, in situ hybridization for EBERs and biopsy for histological study should be performed to confirm the diagnosis.

References

1. Begin LR, Eskandari J, Joncas J, *et al*. Epstein-Barr virus related lymphoepithelioma-like carcinoma of lung. J Surg Oncol 1987; 36(4): 280-3.
2. Ho JC, Wong MP, Lam WK. Lymphoepithelioma-like carcinoma of the lung. Respirology 2006; 11(5): 539-45.
3. Brambilla E, Travis WD, Colby TV, *et al*. The new World Health Organization classification of lung tumours. Eur Respir J 2001; 18(6): 1059-68.
4. Ooi GC, Ho JC, Khong PL, *et al*. Computed tomography characteristics of advanced primary pulmonary lymphoepithelioma-like carcinoma. Eur Radiol 2003; 13(3): 522-6.
5. Chow LT, Chow WH, Tsui WM, *et al*. Fine-needle aspiration cytologic diagnosis of lymphoepithelioma-like carcinoma of the lung. Report of two cases with immunohistochemical study. Am J Clin Pathol 1995; 103(1): 5-40.
6. Eckardt J. Endobronchial ultrasound-guided transbronchial needle aspiration of lesions in mediastinum. J Thorac Dis 2010; 2(3): 125-8.
7. Mukhopadhyay S, Katzenstein AL, Subclassification of non-small cell lung carcinomas lacking morphologic differentiation on biopsy specimens: Utility of an immunohistochemical panel containing TTF-1, napsin A, p63, and CK5/6. Am J Surg Pathol 2011; 35(1): 15-25.
8. Liang Y, Wang L, Zhu Y, *et al*. Primary pulmonary lymphoepithelioma-like carcinoma: Fifty-two patients with long-term follow-up. Cancer 2012. [Epub ahead of print]
9. Hayashi T, Haba R, Tanizawa J, *et al*. Cytopathologic features and differential diagnostic considerations of primary lymphoepithelioma-like carcinoma of the lung. Diagn Cytopathol 2011. [Epub ahead of print]
10. Chan AT, Teo PM, Lam KC, *et al*. Multimodality treatment of primary lymphoepithelioma-like carcinoma of the lung. Cancer 1998; 83(5): 925-9.
11. Han AJ, Xiong M, Gu YY, *et al*. Lymphoepithelioma-like carcinoma of the lung with a better prognosis. A clinicopathologic study of 32 cases. Am J Clin Pathol 2001; 115(6): 841-50.

診斷肺原發類淋巴上皮細胞癌上的陷阱－病例報告與文獻回顧

吳宜謀　沈光漢　許正園

肺原發類淋巴上皮細胞癌是一少見的肺癌。診斷需要組織切片來做免疫組織化學染色。其預後比其他的非小細胞肺癌好。我們報導一個 60 歲男性表現出肺中心部腫瘤併肋膜腔積液。氣管內視鏡超音波經氣管細針抽吸得到的少量細胞，形態學上像鱗狀上皮細胞癌。但經胸腔鏡切片發現高惡性度細胞排列成實質片狀，有不等的淋巴球浸潤且雜交檢測 EB 病毒編碼的 RNA 發現 EB 病毒基因在癌細胞核中。診斷為肺原發類淋巴上皮細胞癌且病人接受鉑金類為主的化學藥物治療。*(胸腔醫學 **2013; 28: 38-43**)*

關鍵詞：肺原發類淋巴上皮細胞癌（LELC），氣管內視鏡超音波經氣管細針抽吸，鱗狀上皮細胞癌，診斷

台中榮民總醫院　內科部　胸腔內科
索取抽印本請聯絡：沈光漢醫師，台中榮民總醫院　內科部　胸腔內科，台中市中港路三段 160 號

A Primary Endobronchial Schwannoma Coexisting with an Ipsilateral Lung Adenocarcinoma: A Case Report and Literature Review

Po-Chiang Chan, Chun-Chi Chang, Ching-Hsiung Lin

Primary endobronchial schwannomas are relatively rare, benign tumors of neurogenic origin. Their presence within the bronchus may lead to cough, hemoptysis, dyspnea and obstructive pneumonia. We present the case of an 83-year-old man with a primary endobronchial schwannoma simultaneously occurring with an ipsilateral bronchogenic adenocarcinoma, and review the literature on primary endobronchial schwannomas. To date, primary endobronchial schwannomas coexisting with lung adenocarcinomas have not been reported, and their relationship is still unknown. We should always keep in mind that endobronchial benign tumors may mimic endobronchial involvement of malignancies. Bronchofiberscopic examination with biopsy is warranted for any endobronchial tumors, and will have an important influence on the staging, treatment, and outcome of coexisting cancers. ***(Thorac Med 2013; 28: 44-50)***

Key words: endobronchial schwannoma, lung adenocarcinoma

Introduction

Most endobronchial tumors, including bronchogenic carcinomas and endobronchial metastases from other origins such as colon, breast, and renal carcinomas, are malignant in nature [1]. Benign endobronchial tumors are quite rare, accounting for approximately 1.9% of all lung tumors, and the majority of benign endobronchial tumors are hamartomas [2]. Unlike malignancies, benign endobronchial tumors are slow-growing and present few symptoms until the consequence of bronchial obstruction occurs. Radiologic features are often normal or nonspecific, and many of the lesions are detected incidentally at bronchoscopy performed for other reasons.

Schwannomas, also called neurilemmomas, are relatively rare benign tumors, accounting for less than 0.2% of pulmonary neoplasms [3]. However, schwannomas found in an endobronchial location are extremely rare. We present a case of primary endobronchial schwannoma coexisting with a bronchogenic adenocarcinoma

Division of Chest Medicine, Department of Internal Medicine, Changhua Christian Hospital, Changhua, Taiwan, ROC

Address reprint requests to: Dr. Chun-Chi Chang, Division of Chest Medicine, Department of Internal Medicine, Changhua Christian Hospital, Changhua, Taiwan, ROC, Changhua Christian Hospital, No.135 Nanshiao Road, Changhua City, 500, Taiwan

in the ipsilateal lung. The association between a benign endobronchial schwannoma and a malignant lung adenocarcinoma is still unclear.

Case Report

An 83-year-old man who had experienced chronic cough for a long time was an active smoker with a smoking history of 120 pack-years. He had been healthy and had no recent discomfort. The past and family histories were also unremarkable. He was referred for expert opinions because of an accidental abnormal finding on chest X-ray (Figure 1). The plain film revealed a 4-cm-sized lobulated soft tissue shadow in the right parahilar region; a lung neoplasm was highly suspected. He had stable vital signs and no abnormal findings on physical examination. Hemogram and biochemical profiles revealed mildly normocytic anemia and mild impaired renal function. We arranged a chest computed tomography (CT) scan with contrast, which showed an irregular heterogeneous low density lesion about 34 mm in length in the right middle lobe, without evidence of an endobronchial lesion (Figure 2) showed as figure 2. There were no enlarged lymph nodes in the neck and mediastinum. Suspecting lung cancer in the right middle lobe, we performed a bronchofiberscopy to obtain the definite diagnosis, if possible. There was no visible endobronchial lesion in the right middle bronchus, but we accidentally detected a yellow-tan, small polyp-

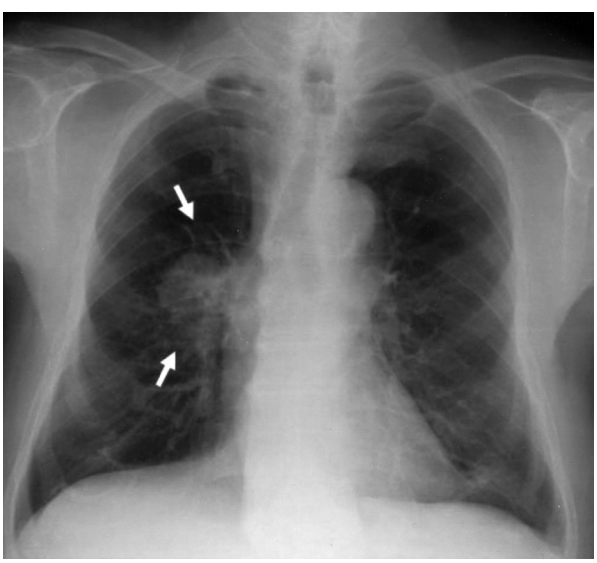

Fig. 1. Chest plain film shows a 4-cm-sized lobulated soft tissue shadow in the right parahilar region (arrows).

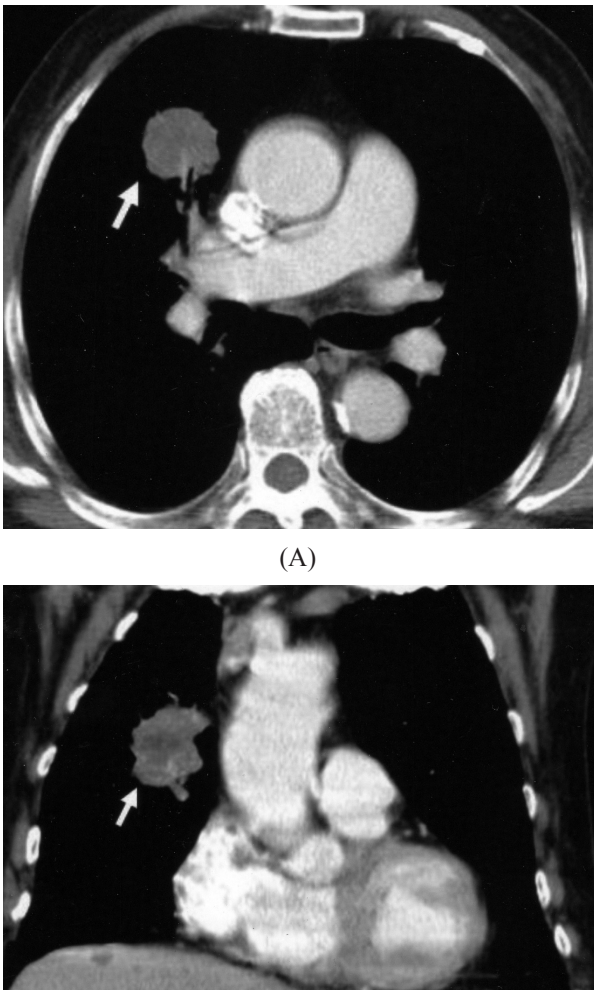

(A)

(B)

Fig. 2. Chest computed tomography shows an irregular heterogeneous low-density lesion about 34 mm in the right middle lobe, without evidence of an endobronchial lesion (arrow).

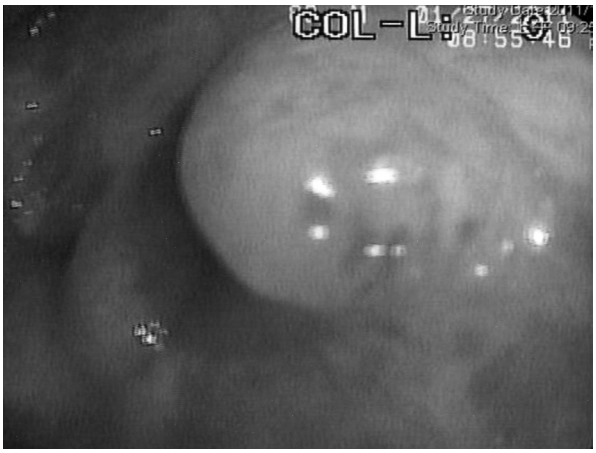

Fig. 3. Bronchofiberscopy shows a yellow-tan, small polypoid, sessile endobronchial lesion in the orifice of the right B2 bronchus.

oid, sessile endobronchial lesion in the orifice of thr right B2 bronchus (Figure 3) Bronchofiberscopic biopsy was done at that time. In the microscopic examination, a schwannoma with proliferation of spindle cells in fascicles in the bronchial wall was found (Figure 4A). Neither mitosis nor necrosis was identified, which suggested a benign tumor. The immunohistochemical stain was positive for S-100 (Figure 4B), and negative for desmin and CD117. We arranged CT-guided lung biopsy for the irregular heterogeneous mass in the right middle lobe to confirm the histological type. Lung adenocarcinoma with the features of nested tumor cells in a fibrotic background with focal tumor necrosis was finally diagnosed. The lung adenocarcinoma was stage Ib, and consisted of T2aN0M0. Because of his age and the high anesthesia risk, the patient and his family refused our advice of a right middle lobectomy and right B2 sleeve segmentectomy. He died 5 months later due to progression of the lung cancer.

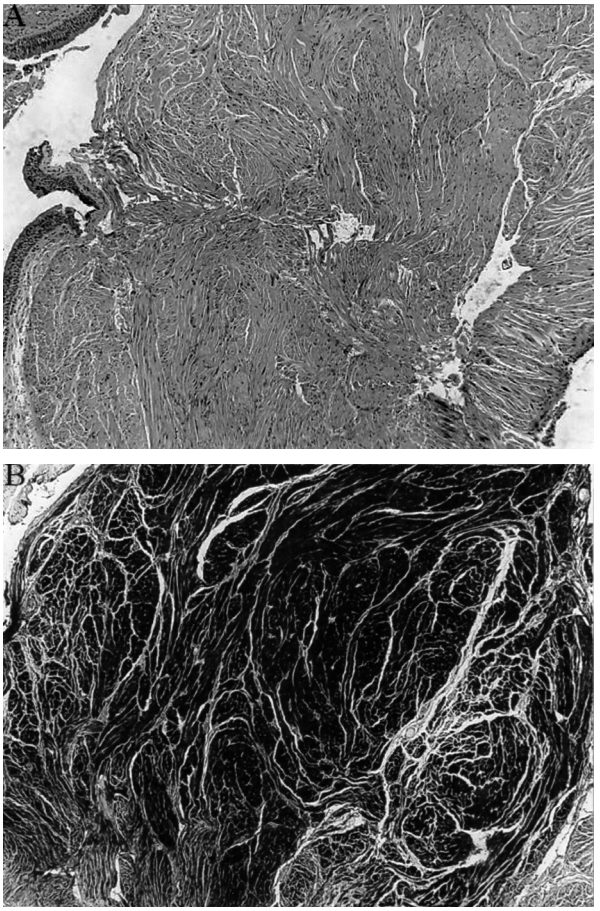

Fig. 4. (A) Schwannoma with proliferation of spindle cells in fascicles in bronchial wall (hematoxylin & eosin stain). (B) Immunohistochemical stain was positive for S-100.

Discussion

The most common neurogenic tumors are neurofibromas that are predominantly associated with neurofibromatosis of Von Recklinghausen's disease [4], and the second most common types are schwannomas with rare malignant transformation [5], accounting for 25% of all intrapulmonary neurogenic tumors [6]. Benign endobronchial tumors can be divided into 3 groups based on origin: mesenchymal, submucosal and surface epithelial (Table 1) [7]. Endobronchial schwannomas are extremely

Table 1. Three Classifications of Benign Endobronchial Tumors

Mesenchymal Origin
Hamartoma
Lipoma
Chondroma
Leiomyoma
Granular cell tumor
Neurogenic tumors
Submucosal Origin
Mucous gland adenoma
Pleomorphic adenoma
Surface Epithelial Origin
Juvenile papillomatosis
Solitary squamous papilloma
Columnar cell papilloma
Fibroepithelial polyp

Table 2. Indications of Surgery for Patients with Endobronchial Neurogenic Tumors

1. Difficulty in making a definite diagnosis and a possible complication with a malignant tumor
2. Peripheral destructive lung disease due to long-term atelectasis or pneumonia
3. Extrabronchial growth
4. Expected technical difficulties during the bronchoscopic procedure due to the multidirectional development of the tumor.

uncommon benign tumors of mesenchymal origin. They have been reported in children and adults, with a predilection for women [8]. The first case was described in 1989 by Feldhaus *et al*. [9]. A review of the literature from 1980 to 2011 disclosed only 28 cases of benign endobronchial schwannomas [4-5,9-22]. Among these publications, there were no reports of a benign endobronchial schwannoma coexisting with a lung adenocarcinoma.

A delayed diagnosis of endobronchial schwannomas usually occurs because of unapparent symptoms, and nonspecific findings on imaging. Endobronchial schwannomas are often well encapsulated, benign tumors arising from peripheral nerves. Nevertheless, multiple lesions at 2-3 different sites in a single patient have also been reported [13,16,22]. Kasahara *et al*. divided these tumors into central types and peripheral types, based on their location [12]. Central-type tumors that are located in the trachea or proximal bronchus are visible directly by bronchofiberscopy, but peripheral-type tumors are not. This classification is closely associated with the symptoms, diagnosis and management of this disease. Bronchofiberscopic examination is warranted if endobronchial lesions are suspected clinically or there is radiological evidence. In our experience, it is difficult to distinguish endobronchial schwannomas from endobronchial involvement of lung cancer using bronchofiberscopy. The definite diagnosis is based on histopathological examination. The presence of typical Antoni A or Antoni B formations on hematoxylin-eosin stain and positive S-100 immunoperoxidase stain is strongly suggestve of a schwannian origin of the neoplasm, and confirms the diagnosis [7].

At present, there is no direct association between endobronchial schwannomas and other diseases, such as COPD, asthma, kidney diseases, liver diseases, or immunocompromised conditions. The relationship between endobronchial schwannomas and cigarette smoking is unproven. Harada *et al*. suggested multiple endobronchial lesions might be caused by the proliferation of Schwann cells as a resulti of cigarette smoking, followed by inflammation of the bronchial mucosa [13]. However, the relationship between endobronchial schwannomas and lung cancer is still equivocal. This report was the first case of primary endobronchial schwannoma simultaneously occurring with an ipsilat-

eral bronchogenic adenocarcinoma in our hospital. As previously mentioned, the patient had an active smoking history, with 120 pack-years of tobacco exposure. Therefore, cigarette smoking may play an important role in the relationship between endobronchial schwannomas and bronchogenic adenocarcinomas.

Management approaches for benign endobronchial schwannomas vary. Although the standard therapy has been surgical resection, bronchoscopic electrical snaring and Nd-YAG laser abrasion have been considered as the first choice recently for symptomatic mass lesions [14]. Complications related to the bronchoscopic procedure, such as pneumomediastinum, pneumothorax, uncontrolled bleeding, air embolism, and cicatricial injury, are uncommon [23]. There is still a possibility of local recurrence for a long period after bronchoscopic resection, and surgery should be chosen in that case [12]. The traditional surgical procedures have been sleeve segmentectomy, pneumonectomy, or lobectomy, depending on the extent of the lesion, the location, and the condition of the distal airway. The indications for surgery in patients with endobronchial neurogenic tumors are listed in Table 2 [14]. For asymptomatic lesions without significant airway obstruction, the "wait and watch" with long-term follow-up approach may be appropriate [2]. For patients such as ours with coexistence of an endobronchial schwannoma and ipsilateral early-stage lung cancer, surgical resection of both tumors is indicated, as long as there is adequate pulmonary function. The prognosis of these patients is generally good after operation.

To sum up, endobronchial schwannomas are extremely rare, and with various clinical manifestations depending on the tumor size and location. Unapparent symptoms and nonspecific findings on imaging usually lead to delayed diagnosis. We have described the first case of a primary endobronchial schwannoma coexisting with an ipsilateral lung adenocarcinoma. We must keep in mind that benign endobronchial tumors may mimic endobronchial involvement of malignancies. Bronchofiberscopic biopsy is always recommended for the definite staging of coexisting lung adenocarcinoma. Surgical resection of both tumors is the best choice in patients with an ipsilateral early-stage lung cancer.

References

1. Kiryu T, Hoshi H, Matsui E, *et al*. Endotracheal/endobronchial metastases: clinicopathologic study with special reference to developmental modes. Chest 2001; 119(3): 768-75.
2. Shah H, Garbe L, Nussbaum E, *et al*. Benign tumors of the tracheobronchial tree. Endoscopic characteristics and role of laser resection. Chest 1995; 107(6): 1744-51.
3. Roviaro G, Montorsi M, Varoli F, *et al*. Primary pulmonary tumours of neurogenic origin. Thorax 1983; 38(12): 942-5.
4. Chen SR, Chen MH, Ho DM, *et al*. Massive hemoptysis caused by endobronchial schwannoma in a patient with neurofibromatosis 2. Am J Med Sci 2003; 325(5): 299-302.
5. Nasiri H, Zeki AA, Albertson TE. A rare diagnosis: Endobronchial schwannoma. J Respir Dis 2010 Jan 4.
6. Bartley TD, Arean VM. Intrapulmonary neurogenic tumors. J Thorac Cardiovasc Surg 1965; 50: 114-23.
7. Wilson RW, Kirejczyk W. Pathological and radiological correlation of endobronchial neoplasms: Part I, Benign tumors. Ann Diagn Pathol 1997; 1(1): 31-46.
8. Righini CA, Lequeux T, Laverierre MH, *et al*. Primary tracheal schwannoma: one case report and a literature review. Eur Arch Otorhinolaryngol 2005; 262(2): 157-60.
9. Feldhaus RJ, Anene C, Bogard P. A rare endobronchial neurilemmoma (schwannoma). Chest 1989; 95(2): 461-2.
10. Higashimoto Y, Ohata M, Kobayashi H, *et al*. A case of primary intrapulmonary benign schwannoma. Nihon Kyo-

bu Shikkan Gakkai Zasshi 1991; 29(3): 360-4.
11. Kilani T, Zaimi M, Labbene N, *et al*. Endobronchial neurogenic tumors. Ann Chir 1992; 46(8): 742-7.
12. Kasahara K, Fukuoka K, Konishi M, *et al*. Two cases of endobronchial neurilemmoma and review of the literature in Japan. Intern Med 2003; 42(12): 1215-8.
13. Harada T, Yamazaki K, Ogura S, *et al*. Multiple endobronchial schwannomas arising at the bronchial spur of two different sites. J Bronchol 2003; 10(3): 195-7.
14. Suzuki H, Sekine Y, Motohashi S, *et al*. Endobronchial neurogenic tumors treated by transbronchial electrical snaring and Nd-YAG laser abrasion: report of three cases. Surg Today 2005; 35(3): 243-6.
15. Oxner CR, Shinners MJ, Godin DA, *et al*. Obstructing tracheobronchial schwannoma. J La State Med Soc 2005; 157(3): 159-61.
16. Bircan A, Kapucuoglu N, Ozturk O, *et al*. Bilateral benign endobronchial schwannomas. Ann Saudi Med 2007; 27(5): 375-7.
17. Nakamura R, Ishikawa S, Sakai M, *et al*. Increased fluorodeoxyglucose-uptake in positron emission tomography with an endobronchial schwannoma occluding the left main stem bronchus. J Thorac Oncol 2009; 4(9): 1183-4.
18. Onal M, Ernam D, Atikcan S, *et al*. Endobronchial schwannoma with massive hemoptysis. Tuberk Toraks 2009; 57(1): 89-92.
19. Stouffer CW, Allan RW, Shillingford MS, *et al*. Endobronchial schwannoma presenting with bronchial obstruction. Interact Cardiovasc Thorac Surg 2009; 10(1): 133-4.
20. Takeda S, Hashimoto T, Kusu T, *et al*. Management and surgical resection for tracheobronchial tumors: institutional experience with 12 patients. Interact Cardiovasc Thorac Surg 2007; 6(4): 484-9.
21. Tansel T, Toker A, Yilmazbayhan D, *et al*. Primary endobronchial schwannoma. J Pediatr Surg 2010; 45(11): 2241-3.
22. Dumoulin E, Gui X, Stather DR, *et al*. Endobronchial schwannoma. J.Bronchol & Intervent Pulmonol 2012; 19(1): 75-7.
23. Choi JC, Yu CM, Ryu YJ, *et al*. The role of endoscopic surgery for completely obstructive endobronchial benign tumor. Korean J Intern Med 2006; 21(1): 15-9.

原發性支氣管內許旺細胞瘤併存同側肺腺癌：病例報告與文獻回顧

詹博強　張竣期　林慶雄

原發性支氣管內許旺細胞瘤是相對罕見的神經原性良性腫瘤。生長於氣管內可能導致咳嗽、咳血、呼吸困難與阻塞性肺炎。我們報告一位 83 歲男性同時存在原發性支氣管內許旺式細胞瘤與同側肺腺癌，並整理回顧支氣管內許旺式細胞瘤的相關文獻。就我們所知，文獻中未曾有與同側肺腺癌併存之支氣管內許旺細胞瘤的個案報告，而兩者之間的相關性依然未知。我們必須留意支氣管內良性腫瘤可能相似於氣管內轉移之惡性腫瘤的情形，因此針對支氣管內腫瘤進行軟式支氣管鏡切片是必要的，對於併存之癌症的分期、治療及預後有重要的影響。*(胸腔醫學 **2013; 28: 44-50**)*

關鍵詞：支氣管內許旺細胞瘤，肺腺癌

財團法人彰化基督教醫院　內科部　胸腔內科
索取抽印本請聯絡：張竣期醫師，財團法人彰化基督教醫院　內科部　胸腔內科，彰化市 500 南校街 135 號

Obstructive Sleep Apnea and Hypopnea Syndrome Originating from an Unusual Anatomical Obstructive Site – A Case Report

Ling-I Chen, Ching-Ping Wang*, Wei-Chang Huang, Ming-Feng Wu, Jeng-Yuan Hsu

Bilateral vocal cord palsy is not an uncommon complication in patients who have experienced neck or thoracic surgery. We describe a male patient who had a past history of thyroid cancer with mediastinum invasion and recurrent laryngeal nerve impairment. Post-thyroidectomy flexible laryngoscope examination revealed bilateral vocal cord palsy. He was referred to the sleep outpatient services due to the new onset of loud snoring when sleeping following the tracheostomy decannulation. Full-night polysomnography (PSG) showed severe obstructive sleep apnea and hypopnea syndrome (OSAHS), and flow-volume loop revealed variable extra-thoracic upper airway obstruction. The level of larynx abnormality contributing to OSAHS has not been clearly determined until now. We present this case to emphasize that laryngeal examinations and flow-volume loop should be implemented in patients with a history of neck or thoracic surgery and a new onset of loud snoring. ***(Thorac Med 2013; 28: 51-56)***

Key words: vocal cord palsy, obstructive sleep apnea and hypopnea syndrome

Introduction

Snoring is an important indicator of apnea/hypopnea. Most snorers suffer from moderate to severe obstructive sleep apnea and hypopnea syndrome (OSAHS), although not all of them necessarily have OSAHS. There are several anatomic abnormalities that are responsible for OSAHS, including nasal obstruction, adenotonsiller enlargement, macroglossia, low positioning of the hyoid bone, and excessive length of the soft palate [1-5]. Herein, we present a patient with severe OSAHS due to bilateral vocal cord palsy -- an unusual case.

Case Report

A 61-year-old man had a past history of thyroid cancer with mediastinum invasion and recurrent laryngeal nerve impairment. He was referred to the sleep outpatient services for evaluation of the new onset of nocturnal loud snoring following tracheostomy decannulation that was noted by his sleep partner.

Division of Chest Medicine, Department of Internal Medicine, Taichung Veterans General Hospital, Taichung, Taiwan; *Department of Otorhinolaryngology, Taichung Veterans General Hospital, Taichung, Taiwan
Address reprint requests to: Dr. Wei-Chang Huang, Division of Chest Medicine, Department of Internal Medicine, Taichung Veterans General Hospital, Address: 160, Sec. 3, Taichung Port Road, Taichung, Taiwan 40705

The patient underwent total thyroidectomy for thyroid cancer initially. Post-thyroidectomy flexible fiberoptic laryngoscope examination revealed bilateral vocal cord palsy, and so a tracheostomy bypass was implemented. The patient recovered well during hospitalization, and received tracheostomy replacement, including fenestrated uncuffed tracheostomy and corking tracheostomy, and swallowing training. The patient tolerated the procedures well, without easily choking. Three months after discharge, follow-up flexible fiberoptic laryngoscopy revealed no changes in the bilateral vocal cord palsy. However, tracheostomy decannulation was carried out at the patient's request since there were no respiratory distress symptoms. A new onset of loud nocturnal snoring was noted by his sleep partner following tracheostomy decannulation. Full-night polysomnography (PSG) indicated severe OSAHS with a respiratory disturbance index of 34.3/hour (Figure 1). Therefore, he was referred to our sleep outpatient services by the otorhinolaryngology department physician.

At the sleep outpatient services, physical examination revealed the patient had a medium stature, with a height of 166 cm, weight of 63 kg, and body mass index of 22.8 kg/m^2. He exhibited no symptom of respiratory distress. Further examination revealed a harsh, high-pitched, inspiratory-phased breathing sound (stridor) in the neck area. Neither enlarged tonsils nor any

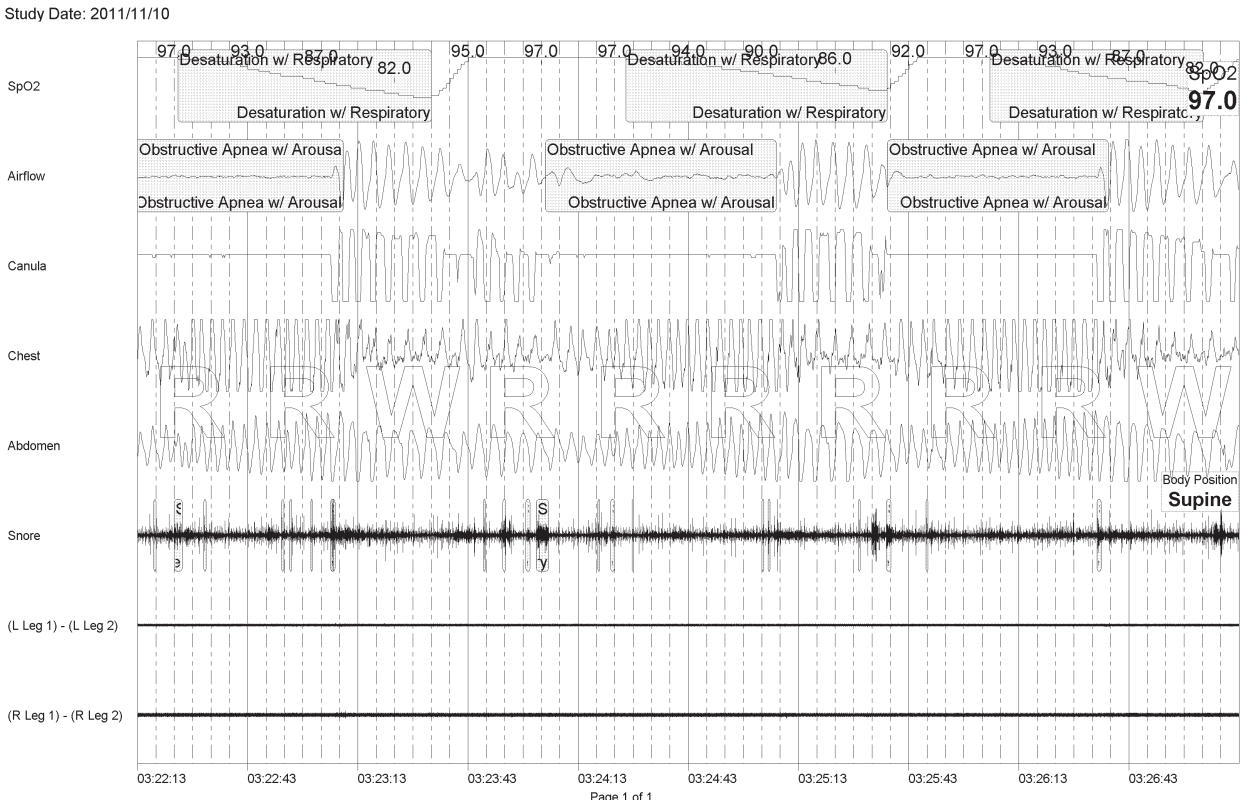

Fig. 1. The typical polysomnographic records of OSAHS in the present case

Name: h,
Gender: Male
Age: 61 Race: Asian
Height(cm): 166
Weight(kg): 63.0

Id: 55968696
Date: 12/20/11
Temp: 16 PBar: 755
Physician:
Result:

F-V LOOP (BTPS)

		PRED	PRE-RX BEST	PRE-RX %PRED	POST-RX BEST	POST-RX %PRED	% CHG
FVC	Liters	3.41	3.97	116			
FEV1	Liters	2.74	2.93	107			
FEV1/FVC	%	81	74				
FEF25-75%	L/sec	2.88	2.34	81			
FEF25%	L/sec	6.74	4.67	69			
FEF50%	L/sec	3.58	3.72	104			
FEF75%	L/sec	1.26	0.69	54			
PEF	L/sec	7.39	5.20	70			
FIVC	Liters	3.41	3.87	114			
FIF50%	L/sec		1.41				
PIF	L/sec		1.48				
FEF/FIF50		<1.00	2.63				
FVL ECode			111010				

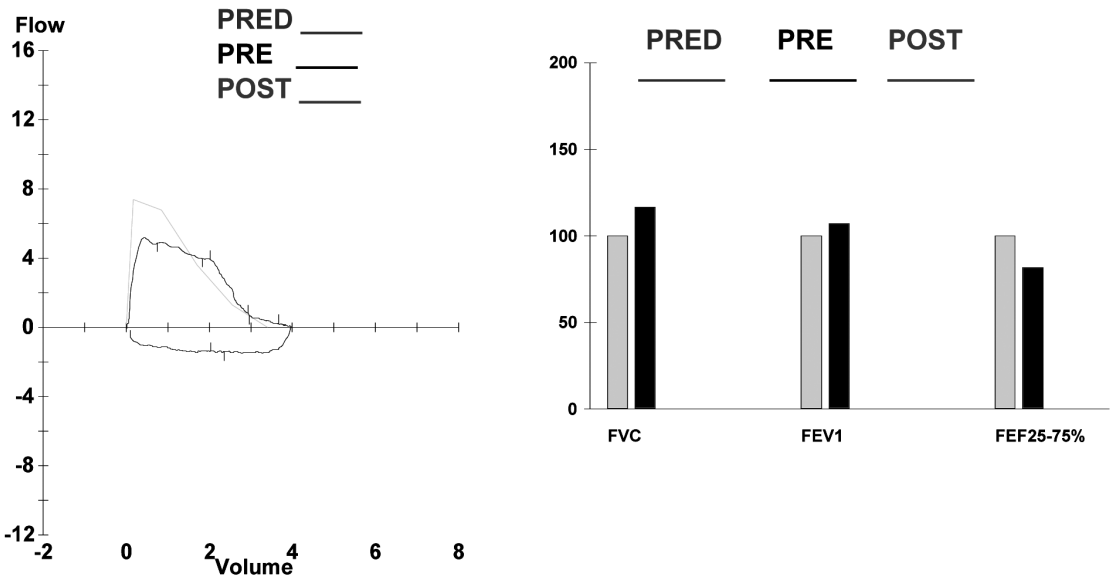

Fig. 2. Flow-volume loop of the present case

other of the usual upper airway anatomic abnormalities responsible for OSAHS were noted. Because of the stridor, a pulmonary function test for the flow-volume loop was performed and indicated variable extra-thoracic upper airway obstruction, which was compatible with the laryngoscopic finding of bilateral vocal cord palsy (Figure 2).

The results suggested that the patient had developed severe OSAHS due to bilateral vocal cord palsy -- an unusual case at an unusual pathogenic anatomical obstructive site. Trache-

ostomy re-cannulation was recommended, but the patient refused because he experienced no respiratory distress symptoms in his daily activities.

Discussion

There are several well-known anatomic abnormalities that are responsible for OSAHS, including nasal obstruction, adenotonsiller enlargement, macroglossia, low positioning of the hyoid bone, and excessive length of the soft palate [1-5]. However, the level of larynx abnormality contributing to OSAHS has not been determined. Congenital or acquired factors causing a collapse or dysfunction of the laryngeal structures and development of sleep-related snoring and OSAHS have been reported [6-10]. Of those, idiopathic or acquired uni- and bilateral vocal cord palsy has resulted in a narrower glottis, higher laryngeal resistance and more negative intralaryngeal pressure followed by complete occlusion at the level of the larynx and OSAHS [7-10]. As in the aforementioned case reports, the OSAHS in our case was caused by acquired bilateral vocal cord palsy following total thyroidectomy. The pathogenesis of OSAHS in patients with vocal cord palsy seems to be similar to that in patients with OSAHS caused by well-known anatomic abnormalities. The difference involves the level of flow limitation. Although the level of larynx abnormality has been postulated to be one of the anatomic abnormalities responsible for OSAHS in only a few case reports, this obstructive anatomic level should be noticeable in patients with a history of neck or thoracic surgery and rapid development of OSAHS.

The upper airway of OSAHS patients behaves similarly to the Starling resistor with a critical closing pressure (P_{crit}) at which the upper airway collapses [11-12]. P_{crit} increases in patients with OSAHS caused by retro-palatal obstruction. Continuous positive airway pressure (CPAP) can alleviate apnea/hypopnea [13-16] by widening the upstream pressure (P_{us}) to a P_{crit} pressure differential. In a similar vein, because of the narrowed supra-glottic or glottic space, laryngeal resistance and P_{crit} increase in patients with OSAHS caused by larynx abnormalities. Thus, CPAP may be effective for patients with OSAHS caused by a larynx abnormality. However, whether CPAP can resolve OSAHS caused by a larynx abnormality should be further investigated.

In patients with OSAHS caused by idiopathic or acquired vocal cord palsy, surgical interventions, including tracheostomy, laterofixation of the vocal cords, and arytenoidectomy could resolve the OSAHS immediately [7-9]. Our patient refused both tracheostomy and CPAP, and continued to report nocturnal loud snoring.

Physical examinations of the upper airway for abnormally abundant soft tissue structures are usually performed routinely and easily for patients with OSAHS at outpatient services. However, laryngeal examinations and the flow-volume loop are easily abridged by sleep specialists because of they are time-consuming and require special equipment. In the present case, the development of a new onset of loud snoring and severe OSAHS caused by bilateral vocal cord palsy following thyroidectomy emphasizes the importance of laryngeal examinations and flow-volume loop in subgroups of OSAHS patients, especially those who have experienced neck or thoracic surgery.

In conclusion, laryngeal examinations and flow-volume loop should be implemented in patients with a history of neck or thoracic sur-

gery and a new onset of loud snoring. Surgical interventions are now the preferred choices of therapy for the level of larynx abnormality contributing to OSAHS. However, whether CPAP can be used as an alternative to resolve OSAHS caused by larynx abnormalities should be further investigated.

References

1. Schwab RJ, Pasirstein M, Pierson R , *et al*. Identification of upper airway anatomic risk factors for obstructive sleep apnea with volumetric magnetic resonance imaging. Am J Respir Crit Care Med 2003; 168: 522-30.
2. Zonato AI, Bittencourt LR, Martinho FL, *et al*. Association of systematic head and neck physical examination with severity of obstructive sleep apnea-hypopnea syndrome. Laryngoscope 2003; 113: 973-80.
3. Gozal D, Kheirandish-Gozal L. The multiple challenges of obstructive sleep apnea in children: morbidity and treatment. Curr Opin Pediatr 2008; 20: 654-8.
4. Kheirandish-Gozal L, Gozal D. The multiple challenges of obstructive sleep apnea in children: Diagnosis. Curr Opin Pediatr 2008; 20: 650-3.
5. Shott SR, Amin R, Chini B, *et al*. Obstructive sleep apnea: should all children with Down syndrome be tested? Arch Otolaryngol Head Neck Surg 2006; 132: 432-6.
6. Chetty KG, Kadifa F, Berry RB, *et al*. Acquired laryngomalacia as a cause of obstructive sleep apnea. Chest 1994; 106: 1898-9.
7. Hoffstein V, Taylor R. Rapid development of OSA following hemidiaphragmatic and unilateral vocal cord paralysis as a complication of mediastinal surgery. Chest 1985; 88: 145-7.
8. Cho GS, Chung YS. A case of nocturnal stridor with combined obstructive sleep apnea caused by bilateral vocal cord palsy. Sleep Med Res 2011; 2: 69-71.
9. Aziz L, Ejnell H. Obstructive sleep apnea caused by bilateral vocal cord paralysis. Ear Nose Throat J 2003; 82: 326-7.
10. Misiolek M, Namyslowski G, Karpe J, *et al*. OSA syndrome and snoring in patients with bilateral vocal cord paralysis. Eur Arch Otol 2003; 260: 183-5.
11. Schwartz AR, Smith PL, Wise RA, *et al*. Introduction of upper airway occlusion in sleeping individuals with subatmospheric nasal pressure. J Appl Physiol 1988; 644: 535-42.
12. Schwartz AR, Gold AR, Schubert N, *et al*. Effect of weight loss on upper airway collapsibility in obstructive sleep apnea. Am Rev Respir Dis 1991; 144: 494-8.
13. Engleman HM, Martin SE, Kingshott RN, *et al*. Randomized placebo controlled trial of daytime function after continuous positive airway pressure (CPAP) therapy for the sleep apnea/hypopnea syndrome. Throax 1998; 53: 341-5.
14. Montserrat JM, Ferrer M, Hernandez L, *et al*. Effectiveness of CPAP treatment in daytime function in sleep apnea syndrome: a randomized controlled study with an optimized placebo. Am J Respir Crit Care Med 2001; 164: 608-13.
15. Patel SR, White DP, Malhotra A, *et al*. Continuous positive airway pressure therapy for treating sleepiness in a diverse population with obstructive sleep apnea: Result of a meta-analysis. Arch Intern Med 2003; 163: 565-71.
16. Weaver TE, Kribbs NB, Pack AI, *et al*. Night-to-night variability in CPAP use over the first three months of treatment. Sleep 1997; 20: 278-83.

罕見解剖構造異常引起阻塞性睡眠呼吸中止症－病例報告

陳鈴宜　王景平 *　黃偉彰　吳明峰　許正園

對於經歷頸部或胸腔手術的患者而言，術後因喉返神經受損引起雙側聲帶麻痺並非少見之併發症。在此病例報告中，一位男性甲狀腺癌病人術後纖維喉鏡檢查發現雙側聲帶麻痺並接受氣切手術。歷經階段性氣切更換與吞嚥訓練後移除氣切。但自氣切移除後，病患開始出現睡眠時打鼾之情況而轉介睡眠門診。經評估後，此病患並無常見引發睡眠呼吸中止症之上呼吸道解剖構造異常。經多頻道睡眠生理檢查顯示有重度阻塞性睡眠呼吸中止症。對於喉部構造異常引起之阻塞性睡眠呼吸中止症目前仍只有少數病例報告發表且治療仍以手術方式為主。我們藉此病例報告提醒對於曾接受頸部或胸腔手術患者新產生之睡眠呼吸中止症候群時，除常見引發之危險因子評估外，纖維喉鏡檢查與肺功能檢查釐清確切阻塞位置是非常重要的。*(胸腔醫學* ***2013; 28: 51-56)***

關鍵詞：聲帶麻痺，阻塞性睡眠呼吸中止症

台中榮民總醫院　內科部　胸腔內科，* 台中榮民總醫院　耳鼻喉部
索取抽印本請聯絡：黃偉彰醫師，台中榮民總醫院　內科部　胸腔內科，台中市西屯區中港路三段 160 號

Pulmonary Physiology before and after Bronchopulmonary Lavage for Pulmonary Alveolar Proteinosis – A Case Report

Chien-Hua Tseng*, Jeng-Yuan Hsu*,**, Pin-Kuei Fu**

Pulmonary alveolar proteinosis (PAP) is a diffuse lung disease characterized by the accumulation of lipoproteinaceous material in the alveoli. Although bronchopulmonary lavage (BPL) is the most widely accepted and effective treatment for patients with moderate to severe hypoxemia, there are few reports about the changes in pulmonary physiology before and after BPL. We report a rare case which was diagnosed as PAP with high plateau pressure. The patient received prolonged mechanical ventilation for 2 months, and was weaned from the ventilator after 2 sequential BPL sessions. We also propose an integrated algorithm which physicians can use when they perform BPL in such critically ill patients. In addition, we present the serial respiratory parameters and serial chest X-rays obtained before and after the BPL to highlight the impact of BPL on PAP in pulmonary physiology. Finally, we provide a figure to illustrate the morphological changes in the pulmonary alveoli and interstitial space, to explain the effect of BPL on PAP. This report is the first on the physiological changes in the lungs and the respiratory parameters before and after the implementation of BPL. ***(Thorac Med 2013; 28: 57-64)***

Key words: bronchopulmonary lavage, pulmonary alveolar proteinosis, plateau pressure, pulmonary physiology

Introduction

Pulmonary alveolar proteinosis (PAP), a rare pulmonary-alveolar disorder, is caused by impaired clearance of surfactants by macrophages, resulting in accumulation of amorphous, lipoproteinaceous acellular material in the lungs [1]. For patients who have moderate to severe symptoms and hypoxemia, bronchopulmonary lavage (BPL) is the most widely accepted and effective form of treatment [2-4]. However, there have been few reports about the changes in pulmonary physiology before and after BPL. Herein, we present a case and highlight the effect of BPL on the lungs in a PAP patient by presenting the serial respiratory

*Division of Chest Medicine, Department of Internal Medicine, Taichung Veterans General Hospital, Taichung, Taiwan; **Division of Critical Care & Respiratory Therapy, Department of Internal Medicine, Taichung Veterans General Hospital, Taichung, Taiwan
Address reprint requests to: Dr. Pin-Kuei Fu, Division of Critical Care & Respiratory Therapy, Department of Internal Medicine, Taichung Veterans General Hospital, 160, Sec. 3, Taichung Port Road, Taichung 40705, Taiwan

parameters and serial chest X-rays obtained before and after performing BPL.

Case Report

A 74-year-old woman had a more than 30-year history of type 2 diabetes mellitus and congestive heart failure. She suffered from progressive shortness of breath with limitation of her daily activities for 3 months. Two months before she was referred to our hospital, she was treated with a serial course of antibiotics due to persistent alveolar patches in the bilateral lung fields. Because of a high-level suspicion of PAP, the patient was then transferred to our hospital for further treatment.

On visual examination, she appeared to be acutely ill with a paradoxical respiratory pattern, and was desaturated (SpO_2=86% with a non-rebreathing mask). She was ventilated mechanically and protective lung strategies were used because of high plateau pressure on the conventional settings. Her ventilator settings were as follows: oxygen fraction (FiO_2) 70%, positive end-expiratory pressure (PEEP) 10 mmHg and preset tidal volume 380 ml (6 ml/kg). Under this setting, her peak airway pressure was 32 mmHg, plateau pressure was 29 mmHg and oxygen saturation was 98%. Broncho-alveolar lavage was performed and the cytology exam confirmed the diagnosis of PAP. BPL is indicated for patients who suffer from PAP with oxygenation failure [2-4]. However, the anesthesiologist suggested using extracorporeal membrane oxygenation (ECMO) due to a high risk of severe hypoxemia during BPL. We then changed the double-lumen endotracheal tube to test the condition of each lung, and also changed the patient's position and found the right lateral decubitus position with the right lung down resulted in better oxygen saturation than the left lung down. Thus, we decided to perform lavage of the left lung first while the patient was in the right lateral decubitus position, and try to conduct an ECMO-free procedure.

In the operating room, we changed the patient's body position to the right lateral decubitus position to ventilate the dependent lung and lavage the independent lung. This required 10 cycles of lavage with a total of 8 liters of saline until the effluent saline became clear. After completing BPL in the left lung, we started to ventilate both lungs. We found the plateau pressure increased from 29 to 34 mmHg after BPL, and the ventilator settings of FiO_2 0.8, PEEP 14 mmHg and tidal volume 360 ml had to be used to keep her oxygenated (Table 1). We tried to perform another BPL in the right lung on the same day, as indicated in a previous report [5], but severe desaturation occurred. Twelve hours after BPL, her net fluid status (I/O) was negative by 319 ml, and the oxygenation status had also improved. We tapered the concentration of O_2 fraction (FiO_2 from 0.8 before BPL to 0.45 after BPL) and kept the protective lung strategy with a low tidal volume of 360 ml. Follow-up serial plateau pressure measurements showed a significant decrease after BPL (from 34 mmHg to 29 mmHg at 12 hours and to 22 mmHg at 48 hours after BPL).

The patient's family would not agree to another BPL due to her bed-ridden status and the desaturation episode during BPL, so she was transferred to a respiratory care ward (RCW) at a local hospital for treatment of chronic respiratory failure. She remained in the RCW for more than 1 month. Weaning from the ventilator was attempted with a pressure support model (PS=12), but it failed; however, her nutrition

Table 1. Ventilator settings and physiological parameters before and after whole lung lavage

	Before 1st lavage	0 hrs	12 hrs	24 hrs	48 hrs	72 hrs	Before 2nd lavage	0 hrs	12 hrs	24 hrs	48 hrs	72 hrs
FiO_2	65	80	45	45	40	40	40	40	40	40	40	40
PEEP	10	14	14	14	10	10	5	5	5	5	5	5
Preset Vt	380	360	360	360	360	360	550	550	550	550	550	550
Peak pr.	32	36	30	29	24	24	24	31	31	32	26	23
Plateau pr.	29	34	27	26	22	22	23	27	24	19	18	16
Mean airway pr.	16	20	20	20	16	16	12	12			8	
SpO_2	98	98	98	99	100	100	100	96	100	100	100	100
I/O			-319		-395	+165			-623		-330	-273

Abbreviation: hrs, hours; Vt, tidal volume; I/O, input/output; pr., pressure.

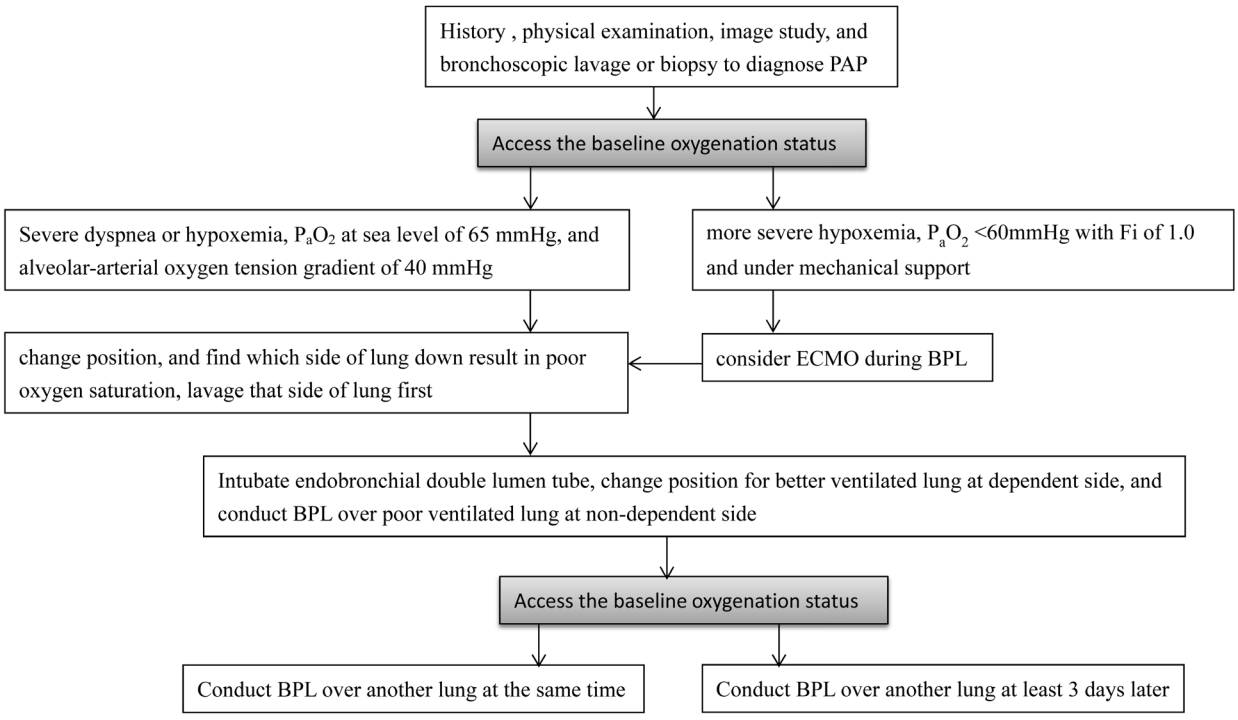

Fig. 1. An integrated algorithm which physicians can use when they perform BPL in critically ill patients. Abbreviation: ECMO, extracorporeal membrane oxygenation

status had improved. Chest X-ray obtained at the RCW showed unilateral infiltration in the right lung, but a clear appearance in the left. She was referred to our hospital again for another lavage of the right lung. A total of 6.5 liters of warm saline was used this time. Once

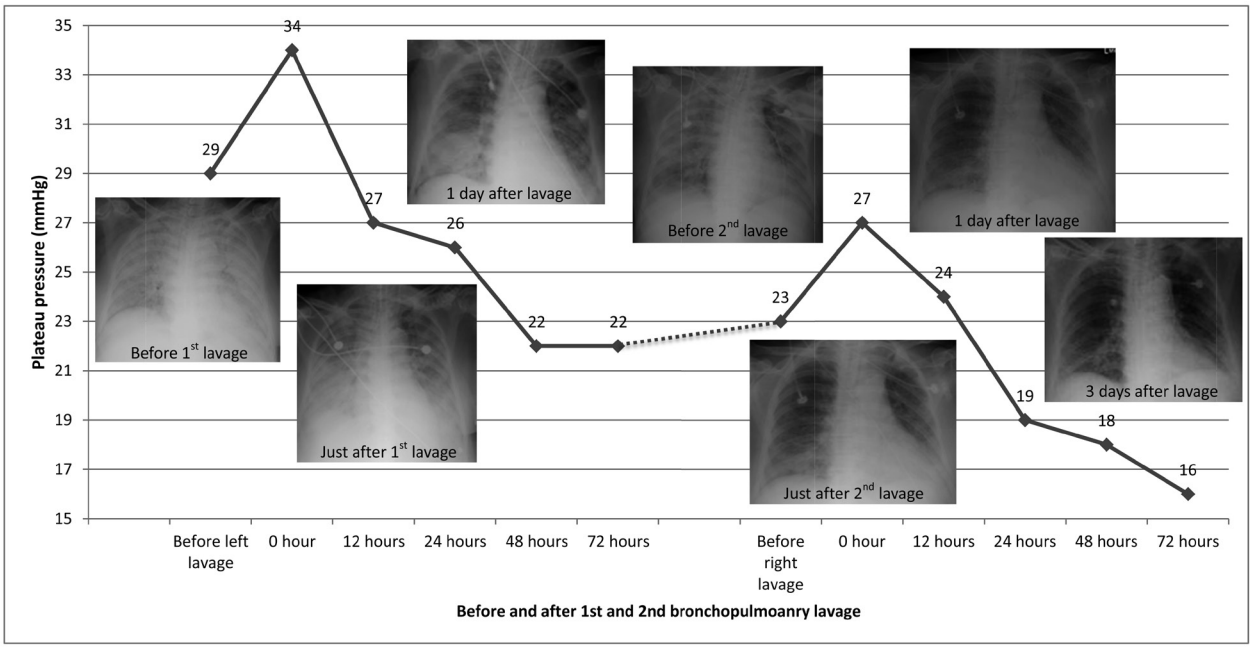

Fig. 2. The changes in serial chest x-ray and plateau pressure before and after bronchopulmonary lavage. The post-lavage chest x-ray showed accentuation of the alveolar opacities on the lavaged side. The lavage-induced acute changes resolved rapidly within 1 to 2 days after lavage. Plateau pressure increased 4~5 mmHg after lung lavage, and decreased 5 mmHg from baseline 48 hours after lung lavage, and even more at 72 hours.

the BPL of the right lung was completed, the plateau pressure increased from 23 mmHg to 27 mmHg, and her oxygen saturation decreased from 100% to 96% under the same ventilator settings (FiO_2=40%, PEEP=5 mmHg, and tidal volume 550 ml). Eight hours later, her oxygen saturation returned to 100%, and the plateau pressure dropped from 27 mmHg to 24 mmHg. We prescribed diuretics to maintain her I/O negative status. The serial plateaus monitored at the 24th, 48th, and 72nd hours after BPL were 19 mmHg, 18 mmHg and 16 mmHg under the same tidal volume of 550 ml (Figure 2). She was successfully weaned from the ventilator 72 hours after the second lavage session.

Discussion

BPL is the most widely accepted and effective treatment for PAP patients with moderate to severe hypoxemia [1-4]. Although the role of BPL in PAP is well recognized, there are some controversies regarding the implementation of BPL, including which lung should be down, which lung should undergo lavage first and whether ECMO is indicated before BPL.

In the traditional performance of BPL of the dependent lung, the patient is placed in the lateral decubitus position and the nondependent lung is ventilated in order to minimize the risk of both lungs being flooded during the procedure. However, this method might be associated with a higher ventilation perfusion mismatch in an already severely hypoxic patient. Therefore,

Timing	Before lavage	After lavage	3 days after lavage
Morphology	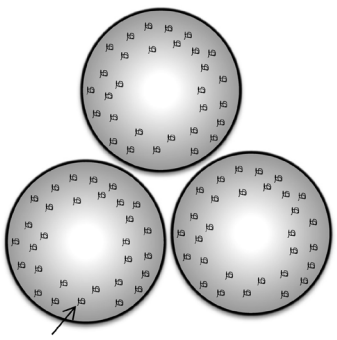	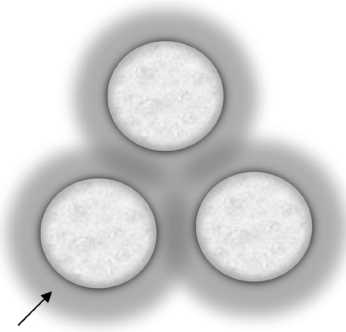	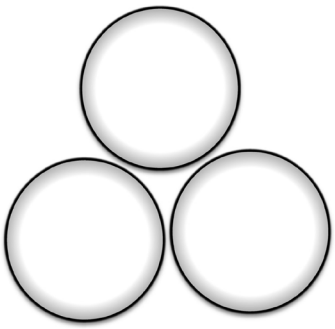
Explain	Alveolar filled with amorphous lipoproteinaceous acellular material(↗)	Alveoli flooding, interstitial edema(↗) leads to poor lung compliance and desaturation	Alveolar space was clear and filled with air

Fig. 3. Alveolar and interstitial morphology before and after lavage.

unlike previous reports, Beccaria and colleagues started by ventilating the dependent lung and conducted lavage in the nondependent lung to obtain a better ventilation perfusion ratio [2,6]. In the present case, that of a patient with severe hypoxemia before BPL, we decided to follow the abovementioned protocol by placing the "good lung down" and performing lavage with the "bad lung up". With this method, we not only performed BPL successfully without ECMO support, but also recovered the instilled normal saline without evidence of leakage at the follow-up chest x-ray (Figure 2).

With regard to which lung should undergo lavage first, there are no arguments in favor of treating the more affected lung first to let the healthier lung provide gas exchange during BPL. However, if both lungs are equally involved, some reports suggested performing left lung lavage first, leaving "the larger right lung" to support better gas exchange during lavage [2]. In our case, we found that PAP involved both lungs equally. To make sure the decision that performing "lavage of the left lung first is better than lavage the right lung first", we had to test the condition of each lung using a double-lumen endotracheal tube to mimic "one-lung ventilation" before BPL was performed.

The issue of the indication for ECMO use in this case was controversial. The anesthesiologist's suggestion to use ECMO in this patient was based on previous reports on ECMO for severe bilateral disease during BPL [7-8]. Patients who needed ECMO during lavage had arterial oxygen saturation of less than 90% under mechanical ventilation at FiO_2 of 1.0 [8]. However, we did not arrange ECMO for this patient because the risk of complications might be high due to her age and multiple comorbidities. Therefore, we proposed an integrated algorithm which physicians can use when they perform BPL in such critically ill patients (Figure 1).

Next, we want to focus on the pulmonary physiology. There are different reasons for the increased plateau pressure before and after BPL. After BPL, instead of lipoproteinaceous material, the alveoli were full of instilled normal saline. However, the high plateau pressure

after BPL could be a transient phenomenon. That is because the clearance rates of both protein and fluid in the flooded alveoli are entirely different. Previous research showed the clearance of protein from flooded alveoli is much slower (1-2% per hour) than that of fluid (10-20% per hour) [9]. The process of alveolar protein clearance could be summarized as follows: proceeding with paracellular diffusion for the short term; then, receptor-mediated clearance, such as albumin-binding protein; and finally, through phagocytosis and catabolism by macrophages for the long term. Macrophages account for most protein clearance from the alveolar spaces, and dysfunction will lead to alveolar proteinosis. On the other hand, the most important factors that drive edema fluid removal from the airspaces are active sodium and chloride transports across the alveolar and distal airway epithelial barriers into the interstitium [10-11]. The uninjured alveolar epithelium plays an important role in rapidly clearing fluid from the airspaces. Even in severe hydrostatic pulmonary edema with an intact alveolar epithelium function, the mean alveolar fluid clearance in the first 4 hours was up to 13% per hour [12]; however, in severe lung injury with alveolar epithelium dysfunction, the mean alveolar fluid clearance in the first 4 hours was only 6% per hour [13]. Since the function of the alveolar epithelium is presumed to be intact in PAP, the finding that the rapid alveolar epithelial fluid clearance rate during the first hour after BPL in PAP was as high as 53±10% is not very surprising [14].

In this case report, we highlighted some problems, such as which lung should be down, which lung should undergo lavage first and whether ECMO is indicated when dealing with severe bilateral PAP patients. We observed severe desaturation and high plateau pressure during and within 12 hours after lavage. However, the hypoxemia was stabilized and plateau pressure returned to a lower level than at baseline 2 to 3 days after lavage. This report is the first to focus on the physiological changes in the lungs and the respiratory parameters before and after the implementation of BPL.

References

1. Trapnell BC, Whitsett JA, Nakata K. Pulmonary alveolar proteinosis. N Engl J Med 2003; 349: 2527-39.
2. Beccaria M, Luisetti M, Rodi G, *et al*. Long-term durable benefit after whole lung lavage in pulmonary alveolar proteinosis. Eur Respir J 2004; 23: 526-31.
3. Claypool WD, Rogers RM, Matuschak GM. Update on the clinical diagnosis, management, and pathogenesis of pulmonary alveolar proteinosis (phospholipidosis). Chest 1984; 85: 550-8.
4. Larson RK, Gordinier R. Pulmonary alveolar proteinosis. Report of six cases, review of the literature, and formulation of a new theory. Ann Intern Med 1965; 62: 292-312.
5. Shah PL, Hansell D, Lawson PR, *et al*. Pulmonary alveolar proteinosis: clinical aspects and current concepts on pathogenesis. Thorax 2000; 55: 67-77.
6. Michaud G, Reddy C, Ernst A. Whole-lung lavage for pulmonary alveolar proteinosis. Chest 2009; 136: 1678-81.
7. Zapol WM, Wilson R, Hales C, *et al*. Venovenous bypass with a membrane lung to support bilateral lung lavage. JAMA 1984; 251: 3269-71.
8. Cohen ES, Elpern E, Silver MR. Pulmonary alveolar proteinosis causing severe hypoxemic respiratory failure treated with sequential whole-lung lavage utilizing venovenous extracorporeal membrane oxygenation: a case report and review. Chest 2001; 120: 1024-6.
9. Hastings RH, Folkesson HG, Matthay MA. Mechanisms of alveolar protein clearance in the intact lung. Am J Physiol Lung Cell Mol Physiol 2004; 286: L679-89.
10. Matthay MA, Folkesson HG, Clerici C. Lung epithelial fluid transport and the resolution of pulmonary edema. Physiol Rev 2002; 82: 569-600.

11. Matthay MA, Robriquet L, Fang X. Alveolar epithelium: role in lung fluid balance and acute lung injury. Proc Am Thorac Soc 2005; 2: 206-13.
12. Verghese GM, Ware LB, Matthay BA, *et al*. Alveolar epithelial fluid transport and the resolution of clinically severe hydrostatic pulmonary edema. J Appl Physiol 1999; 87: 1301-12.
13. Ware LB, Matthay MA. Alveolar fluid clearance is impaired in the majority of patients with acute lung injury and the acute respiratory distress syndrome. Am J Respir Crit Care Med 2001; 163: 1376-83.
14. Chesnutt MS, Nuckton TJ, Golden J, *et al*. Rapid alveolar epithelial fluid clearance following lung lavage in pulmonary alveolar proteinosis. Chest 2001; 120: 271-4.

肺泡蛋白沉積症的支氣管肺泡灌洗前後生理參數變化－病例報告

曾健華 * 許正園 *,** 傅彬貴 **

肺泡蛋白沉積症（PAP）是一種因肺泡累積脂蛋白物質導致瀰漫性肺疾病。對於中度至嚴重症狀和低血氧症患者，雖然支氣管肺泡灌洗是最被廣泛接受和有效的治療，但鮮少文獻討論支氣管肺泡灌洗前後的肺生理變化。我們報告一個病例：肺泡蛋白沉積症併發 2 個月呼吸衰竭，在接受 2 次支氣管肺泡灌洗治療後，成功脫離呼吸器，而我們也提出了一個處理嚴重肺泡蛋白沉積症的流程圖。在病患接受支氣管肺泡灌洗治療前後，我們記錄了呼吸參數及胸部 X 光片來探討支氣管肺泡灌洗對肺泡蛋白沉積症病患的肺部生理影響。最後，我們以繪圖的方式試著去形容肺泡及肺間質在支氣管肺泡灌洗的前後變化。這份報告是第一篇詳細討論支氣管肺泡灌洗前後肺部和呼吸參數的生理變化之相關文獻。*(胸腔醫學* ***2013; 28: 57-64)***

關鍵詞：支氣管肺泡灌洗，肺泡蛋白沉積症

* 台中榮民總醫院　內科部　胸腔內科，** 台中榮民總醫院　內科部　呼吸治療科
索取抽印本請聯絡：傅彬貴醫師，台中榮民總醫院　內科部　呼吸治療科，台中市中港路三段 160 號